Article

Quality Assessment of Groundwater Based on Geochemical Modelling and Water Quality Index (WQI)

Arifullah [1,2], **Huang Changsheng** [1,2,*], **Waseem Akram** [1,2], **Abdur Rashid** [3], **Zahid Ullah** [3,*],
Muddaser Shah [4,5], **Abdulwahed Fahad Alrefaei** [6], **Mohamed Kamel** [7], **Lotfi Aleya** [8]
and Mohamed M. Abdel-Daim [9]

[1] Institute of Geological Survey, China University of Geosciences, 388 Lumo Road, Wuhan 430074, China
[2] Department of Hydrogeology and Environmental Geology, Wuhan Centre of China Geological Survey, Wuhan 430074, China
[3] State Key Laboratory of Biogeology and Environmental Geology & School of Environmental Studies, China University of Geosciences, Wuhan 430074, China
[4] Department of Botany, Abdul Wali Khan University, Mardan 23200, Pakistan
[5] Natural and Medical Sciences Research Center, University of Nizwa, P.O. Box 33, Birkat Al Mauz, Nizwa 616, Oman
[6] Department of Zoology, College of Science, King Saud University, P.O. Box 2455, Riyadh 11451, Saudi Arabia
[7] Department of Medicine and Infectious Diseases, Faculty of Veterinary Medicine, Cairo University, Giza 12211, Egypt
[8] Chrono-Environnement Laboratory, UMR CNRS 6249, Bourgogne, Franche-Comté University, CEDEX, F-25030 Besancon, France
[9] Pharmacology Department, Faculty of Veterinary Medicine, Suez Canal University, Ismailia 41522, Egypt
* Correspondence: 1201990094@cug.edu.cn (H.C.); 2201890048@cug.edu.cn (Z.U.)

Abstract: Potable groundwater contamination through arsenic (As) is a common environmental problem in many developing countries, including Pakistan, with significant human health risk reports. The current research was conducted in District Nankana Sahib, which is a major industrial site in Punjab, Pakistan. According to the Punjab Directorate of Industries in Pakistan, there are more than a thousand industries in this area. These industries produce a lot of waste and effluent, which contaminate the environment with harmful and toxic materials. Continuous irrigation with industrial effluent and sewage sludge may make groundwater sources vulnerable. Therefore, this research was aimed as assessing the hydrochemical profile of groundwater concerning As contamination in the study area using sixty-seven groundwater samples. Multivariate statistical analysis, graphical plots, geochemical modeling, and the water quality index (WQI) were applied to investigate the hydrochemistry of the research area. The outcomes of the WQI revealed that 43% of the samples were of poor quality and not fit for human consumption. About 28% of the groundwater samples showed high arsenic contamination beyond the permitted limit of the World Health Organization (WHO). The piper plot identified three distinct types of water in the research area: calcium, chloride, and calcium-chloride types. The Gibbs diagram illustrated that rock–water interaction influenced the hydrochemistry. Terrigenous sedimentary rocks, such as stream deposits, flood plain deposits, and detrital sedimentary rocks, among other types of sedimentary rocks covered most part the study area. Principal component analysis (PCA) and hierarchical cluster analysis (HCA) indicated that the arsenic in groundwater exhibited a significant positive correlation for pH, Fe and As. Health risk assessments indicated a hazard quotient (HQ) greater than 1, indicating a 28% contribution showing that groundwater ingestion is highly toxic to the local habitats. The results of this study further help in managing future sustainable groundwater management approaches in the Nankana District, Punjab, Pakistan.

Keywords: groundwater; arsenic contamination; water-quality index; geochemical modeling; hydrochemical facies; Nankana District

1. Introduction

Groundwater is an essential source for domestic and industrial purposes. The extraction of this natural resource is highly increased globally due to the rising population and the easy access to new and cheap extraction technologies [1]. A growing trend toward the subsurface disposal of wastes has accelerated the movement of contaminants in groundwater systems in recent years [2]. The groundwater throughout the regions where industry and agriculture have been delegated could be contaminated by a wide range of pollutants. These contaminants include nitrate, sulphate, chloride, toxic organic compounds released by mineral fertilizers and pesticides, pathogens, and sulphate [3,4]. Groundwater contamination is a critical issue, particularly in rapidly developing cities and industrial areas, where untreated industrial wastewater drainage, excessive fertilizers, improper landfills, and agricultural pesticides are comparatively common [5].

Groundwater exposure to arsenic is a severe environmental hazard to human health. Many individuals are exposed to arsenic through the oral ingestion of water [6]. Arsenic concentration in groundwater has been recorded as more than 10 µg/L in different countries throughout the world, such as Spain, Portugal, and Hungary, and particularly in Asian countries, such as Pakistan, China, Iran, India, and Bangladesh [7–9]. As per recent research, human health can even be affected by exposure to arsenic under 10 µg/L; therefore, developed countries are modifying their water treatment plants to provide potable water with lower than 1 µg/L of arsenic [10].

Both geogenic and human activities contribute to arsenic in groundwater. Geogenic sources of arsenic are rock types and sediments, where arsenic occurs naturally as a trace element. Arsenic is typically found in sedimentary or igneous rock, either by itself or in combination with other elements, such as oxygen. Igneous and sedimentary rocks have an average arsenic concentration of 2 mg kg^{-1}. The arsenic concentration in most rocks ranges from 0.5 to 2.5 mg kg^{-1} [11], whereas higher concentrations have been observed in phosphorites and clayey or argillaceous sediments [12,13]. The transportation of arsenic from natural sources into groundwater depends on the type of arsenic, the environment of the aquifer, and the biogeochemical processes. Arsenic is found in more than 200 minerals on the earth's surface. Arsenolite, arsenopyrite (FeAsS), anargite (Cu_3AsS_4), and orpiment are the most common sources of groundwater arsenic pollution. Furthermore, anthropogenic activities, mainly mining arsenic-bearing sulfide, pesticides, and improper landfills, push arsenic into groundwater [14].

In Pakistan, recent studies on groundwater contamination revealed that about 70% of the ground and surface water reservoirs are highly polluted with organic, inorganic, and biological pollutants [15,16]. Approximately 47 million inhabitants in Pakistan belong to those areas, where they rely on consuming tube-well water for drinking and domestic purposes, which may contain As concentrations exceeding 10 µg/L in 50% of the total wells [16,17], and as recorded by [18,19], 17% of people drink water containing above 50 µg/L of As. Only 26% have access to clean water [20]. Most of the regions of the Sindh and Punjab provinces of Pakistan are comprised of alluvial and deltaic deposits of the Quaternary (Pleistocene) age, with thicknesses extending from a few meters to hundreds of meters [21,22]. Furthermore, the groundwater in such regions is polluted with significant levels of arsenic [23]. Previous research has been performed to find fresh water aquifers in the District using the electrical resistivity method [24]. To identify the possible sources of arsenic in the District's groundwater, the aim of this research was (i) to investigate the physicochemical features of the groundwater sources; (ii) to investigate the study area's particular distribution pattern and the amount of arsenic risk to the local population; (iii) to investigate the relationship between arsenic and other groundwater variables, as well as to identify pollutant sources; (iv) to evaluate the suitability of the groundwater for ingestion using the WQI approach.

2. Area and Physiography

The study area (Nankana Sahib District) is in Punjab province, Pakistan, within a latitude of 31.452097 N and a longitude of 73.708305 E (Figure 1). The district has three subdivisions: Shangla Hill, Shah Kot, and Nankana Sahib Tehsil. Geographically, it is situated about 91 km from the west of Lahore and about 75 km from the east of Faisalabad city. The total population of Nankana Sahib is approximately 1,356,774 inhabitants (2017 census report by Pakistan bureau of statistics). Climatically, it lies within the semi-arid climatic zone. In the summer, the temperature reaches 40–45 °C. The temperature in May and June is quite high, while a minimum temperature 22–25 °C is recorded for December and January. The monsoon season begins in June and lasts for around two months. The average rainfall of Nankana Sahib is 635 mm [25]. The soil of Nankana Sahib is fertile. There are three major crops cultivated in the area: wheat, rice and sugarcane [26]. In the District, most inhabitants use groundwater for domestic use; the tube-well density in the entire District is (19,161 in total). In most areas, the depth of the water table is about 7.5 to 9.14 m, which has no difficulty pumping out [27].
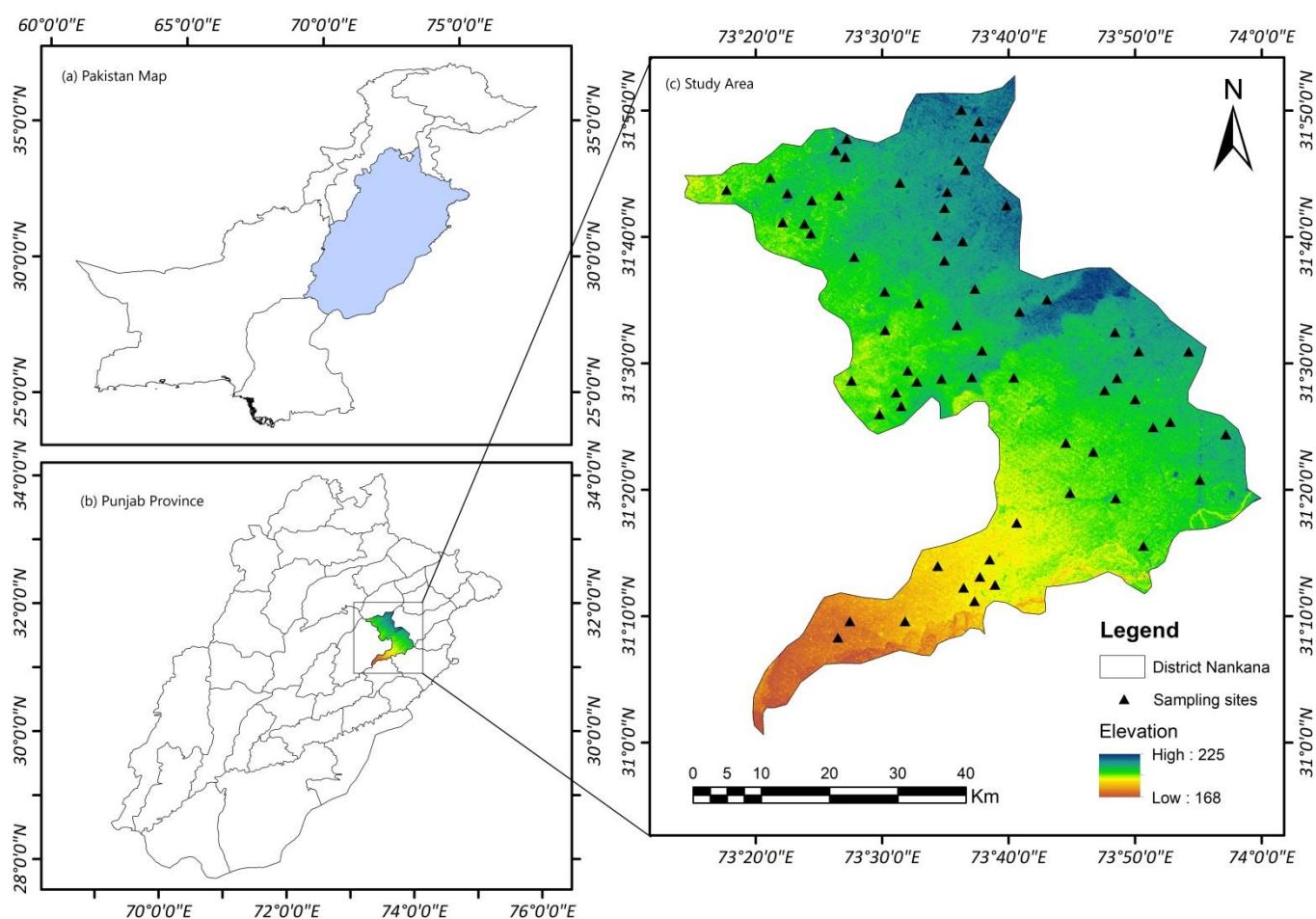
Figure 1. Geographical map of the study area with sample locations.

Geology and Hydrogeology

The soil of Punjab is composed of alluvial materials transported from the Himalayan Mountains by tributaries of the Indus River. Across many aspects, the soils are quite similar throughout the region. They are relatively coarse and medium-textured reddish–brown to greyish–brown soils with high clayey sand and silty sand, which are Precambrian metamorphic and igneous rocks or semi-consolidated tertiary rock covered by quaternary alluvium deposits in the Punjab plains [28].

The district is located between the Ravi River and Chenab's watersheds, also known as Rachna Dhoab. The area is covered with thick alluvial and river deposits. The current study area contains terrigenous sedimentary rocks, such as stream deposits, flood plain deposits, and detrital sedimentary rocks, among other types of sedimentary rocks. Sand and gravels are water-bearing strata. Most aquifers in this area are confined, although certain regions have unconfined aquifers with gravel and pebbles on the surface [24].

Furthermore, the significant sources of aquifer recharge include canals, water channels, and percolation through irrigation and rainfall. The area's water table fluctuates depending on seasonal recharge. Exploratory drilling in the region of the subsurface bedrock in Chaj, Rechna, and Bari Doabs has discovered that the Precambrian underlying rocks are covered by Quaternary alluvium [29]. Sediments range from sandy clay to clayey sand, predominantly grey to brownish grey, in various proportions. Water-bearing strata are sand, gravel, and coarse aggregates. Ravi and Chenab are the two major rivers that drain the area [30,31]. During the summer, the average monthly discharge is around 15–20 times that in the winter. Upstream groundwater seepage is a common cause of reduced flow from December to the middle of March. During the spring melt of the Himalayan snow, river levels often rise sharply, reaching their highest point in July or August, when the monsoon rains arrive [32].

3. Methodology

3.1. Sampling and Analysis

A total of 67 groundwater samples were taken from different sites in July 2018 in the entire District. Samples were taken for physicochemical analysis from existing tube wells, hand pumps, motor pumps, and the water supply scheme in the District. Pre-cleaned polystyrene bottles were used to store the samples. Samples were taken after the bore holes were purged through continues pumping to remove the stagnant water's impact. On-site measurements were performed for the variables, such as pH, electrical conductivity (EC), temperature, and total dissolved solids (TDS) measurements. For further analysis, the samples were sent to the Pakistan Council of Research in Water Resources (PCRWR) laboratory. The evaluation of water samples for aesthetic, physicochemical, and bacteriological characteristics was carried out according to the American Public Health Association (APHA). The pH and TDS were measured by a pH meter (Hanna Instrument, Model 8519, Italy) and the 2540 C standard method (2012), respectively. For alkalinity (carbonate and bicarbonate), the 2320 standard method (2012) was employed. To measure arsenic levels, the AAS Vario 6, Analytik Jena AG Germany (3111B APHA) 2012 technique was utilized. Nitrate (NO_3^- as N) was determined by using Cd-reduction (Hach-8171) using the spectrophotometer technique [33]. The amounts of calcium, chloride, magnesium, and sulfate were determined using the standard procedures 3500-Ca-D (2012), titration (Silver Nitrate) (2012), 2340-C (2012), and SulfaVer4 (Hach-8051) (2012) by a spectrophotometer. Flame photometer PFP7, UK method was utilized to quantify potassium and sodium. Furthermore, fluoride (F), iron (Fe), and turbidity were measured using 4500-FC Ion-Selective Electrode Method Standard (2012), Ferro Ver Method (HACH Cat. 21057-69), and turbidity meter, LaMotte (Model 2008, USA) method, respectively [34]. The charge balance error (CBE) was estimated to ensure that water samples were accurately analyzed, within ±10% acceptable limits [35]. The following equations were used to calculate charge balance error, where cations, as well as anions, were represented in meq/L [36].

$$\text{CBE\%} = \frac{\sum \text{cations} - \sum \text{anions}}{\sum \text{cations} + \sum \text{anions}} \times 100 \tag{1}$$

3.2. Multivariate Statistical Analysis

3.2.1. Correlation Analysis

Correlation analysis is generally utilized to identify the correlation between two variables. We employed Pearson's correlation to better comprehend the correlation between Hydrochemical parameters, as well as the effect of associated parameters.

3.2.2. Hierarchical Cluster Analysis (HCA)

Hierarchical Cluster analysis is a widely used statistical tool for organizing data based on their characteristics. It divides objects into clusters, so components with the same group show the most similar characteristics [37]. Ward's method of joining rules and the Euclidean distance were applied to estimate the correlation among water quality measures. The cluster analysis results were then employed to deduce the hydrochemical procedures which occurred in the research area [38].

3.2.3. Principle Component Analysis (PCA)

PCA is widely used to reduce huge datasets with minimum loss of information [39]. PCA was calculated with SPSS software (version 25) to clarify the cluster analysis results and the factors that described the variances in most groundwater quality data [40].

3.3. Groundwater Type and Classification

Common ion concentrations in groundwater samples are typically represented using the piper plot. The piper plot was constructed to analyze the various factors that influenced the hydrochemistry of the research area. In the Gibbs diagram, cations $Na^+/(Na^+/Ca^{2+})$ and anions $Cl^-/(Cl^- + HCO_3^-)$ were placed against TDS. Microsoft Excel (version 2020) was used to construct the Gibbs plot to identify the controlling mechanisms of groundwater of the research area.

3.4. Geochemical Modeling

Chloro-alkaline indices (CAI-I and CAI-II) and saturation indices were computed to identify the ion exchange processes and the status of saturation of different minerals in the groundwater samples, respectively. PHREEQC interactive software (version 3.1) was employed to calculate the mineral saturation phase [41,42], while the following formulas were employed to compute the chloro-alkaline indices.

$$CAI\text{-}1 = Cl^- \ (Na^+ + K^+)/Cl^- \qquad (2)$$

$$CAI\text{-}2 = Cl^-(Na^+ + K^+)/HCO_3^- + SO_4^{2-} + CO_3^- + NO_3 \qquad (3)$$

3.5. Water Quality Index (WQI)

The water quality index (WQI) was estimated by adopting the weighted arithmetic index technique [43]. The following steps were followed to calculate the WQI.

Step 1: Each sample's Wn factor was determined using the following formula:

$$Wn = \frac{K}{Sn}$$

where Sn = standard desirable value of nth parameters.

$$Wn = 1 \ (unity).$$

K = constant of proportionality.
The value of K = 1; it is a constant value and used to calculate the standard desirable value of each chemical variable.

Step 2: The sub-index (Qn) value was calculated by using the expression

$$Qn = \frac{[(Vn - Vo)]}{[(Sn - Vo)]} \times 100 \tag{4}$$

where
Vn = average concentration of the nth parameter.
Sn = standard desirable value of the nth parameter.
Vo = actual values of the parameters in pure water (generally $V_0 = 0$ for most parameters, except for pH).

$$QpH = \frac{[(VpH - 7)]}{[(8.5 - 7)]} \times 100 \tag{5}$$

Step 3: Step 1 and Step 2 were combined to determine WQI

$$\text{Overall WQI} = \frac{\sum WQn}{\sum Wn} \tag{6}$$

3.6. Heath Risk Assessment

Arsenic can enter the human body in different ways, such as inhalation, dermal exposure, and oral digestion. Among these pathways, direct oral intake is the potential source of human susceptibility to arsenic and heavy metals (more than 90%) [44]. As a result, the acute and cancer risks caused by drinking polluted water containing arsenic were assessed. Exposure risk assessment was utilized to obtain the chronic risk. ADD refers to the average daily arsenic dosage, and it is calculated by applying the formula below:

$$ADD = C \times IR/BW \tag{7}$$

C refers to arsenic concentration (μg/L) in groundwater, IR stands for ingestion ratio (2 L/day), and BW represents body weight (70 kg).

A Health Quotient (HQ) calculation can determine non-carcinogenic health risks triggered by consuming high arsenic water levels [45,46]. The HQ of the study area was calculated utilizing the subsequent equation:

$$HQ = ADD/RFD \tag{8}$$

The oral recommended dosage of 0.3 (μg kg/day) is RFD. It is regarded safe when the risk factor of the sample is less than 1. Samples having hazard quotient values below 1 are considered safe, while those with HQ values greater than 1 may reflect health danger. Furthermore, cancer risk analysis was also measured by employing the below formula

$$CR = ADD \times CSF \tag{9}$$

where CSF stands for the cancer slope factor (1.5 mg/kg/day) [46].

4. Result and Discussion

4.1. Groundwater Hydrochemical Properties

The physicochemical parameters were statistically analyzed and compared with the standard limits of WHO [47]. Table 1 includes each variable's highest and lowest value, mean, and standard deviation. The pH in the research region varied from 7.1 to 8.3, with a median of 7.8. This suggests that the groundwater in the research area is well buffered. The electrical conductivity varied from 160 to 3710 μS/cm, showing a mean of 1572.03 μS/cm, and 59% of the water samples crossed the WHO standards of 1000 μS/cm. Similarly, values of total dissolved solids (TDS) ranged from 1.67 mg/L to 2226 mg/L, having a mean of 954.70 mg/L, where 44% of the water exceeds the standard limit of 1000 mg/L [40,47]. High concentrations of TDS make water saltier, so consuming such water may cause serious health issues, such as gastrointestinal exasperation [48]. The concentrations of

Na^+, Mg^{2+}, and K^+ were in the range of 6–700 mg/L, 5–124 mg/L, and 2.3–95 mg/L, with a median of 242.49, 37.61, and 10.96 mg/L, respectively. All samples of Mg^{2+} and K^+ were within the permissible limit, while 53% of groundwater samples showed high Na^+ concentrations. Dissolution of sodium-containing minerals and anthropogenic activities can contribute to sodium enrichment in groundwater [49]. The concentrations of chloride, sulfate, and phosphate in groundwater were in the range of 2–558 mg/L, 11–472 mg/L, and 0.01–0.35 mg/L, respectively, where 35% of the water samples of chloride, 31% of sulfate, and 50% of phosphate crossed the WHO limit. Phosphate in groundwater could be caused by regional sources, such as sewage interacting with shallow groundwater, agricultural runoff discharge and landfill leachates [50]. Sulfate in groundwater might be caused by sulphide mineral oxidation, weathering of gypsum-bearing rocks ($CaSO_4 2H_2O$), and human inputs, such as industrial waste water and fertilizers [51]. Chloride in groundwater could be derived from a number of sources, including home and municipal pollutants, weathering, and leaching from sedimentary rocks [52]. The content of HCO_3^- ranged from 50 to 945 mg/L, with a mean of 359.55 mg/L, where 43 groundwater samples enriched with HCO_3^- were above the standard limit of WHO. The oxidation of organic substances present in the aquifer yields carbon dioxide, which is most likely the source of bicarbonate in subsurface water [53]. Nitrate and iron concentrations extended from 0.01 to 18 mg/L and 0.03 to 0.95 mg/L, respectively. All NO_3^- and Fe^- samples were under the WHO prescribed range. The primary sources of nitrate contaminants in the groundwater are agricultural runoff, wastewater discharge from sewage water, and the degradation of nitrogenous waste from humans and animals [47]. Table 1 shows descriptive statistics of groundwater variables.

Table 1. Descriptive statistics of groundwater samples variables.

Chemical Parameters	W.H.O Standards	Minimum	Maximum	Mean	St. Deviation	Samples E.P.L	% Of Samples E.P. L
pH	6.5–8.5	7.1	8.3	7.8	0.263	0	0%
EC (µS/cm)	<1000	160	3710	1572.03	974.329	40	59%
TDS (mg/L)	<1000	1.67	2226	954.70	600.374	30	44%
Total hardness (mg/L)	100–500	70	710	294.78	134.199	8	11%
HCO_3^- (mg/L)	150–300	50	945	359.55	179.818	43	64%
Ca^{2+} (mg/L)	75	20	S120	55.19403	20.594	11	16%
F^- (mg/L)	0.6–1.5	0.04	2.5	0.54	0.444	4	5%
Mg^{2+} (mg/L)	30–150	5	124	37.61	24.074	0	0%
Na^+ (mg/L)	50–200	6	700	242.49	191.389	36	53%
K^+ (mg/L)	30–200	2.3	95	10.96	16.303	0	0
Cl^- (mg/L)	250	2	568	195.10	177.986	24	35%
$NO_3(N)$	45	0.01	18	1.59	2.888	0	0%
$PO4^{-3}$ (mg/L)	0.1	0.01	0.35	0.13	0.095	34	50%
SO_4^{2-} (mg/L)	250	11	472	188.45	129.385	21	31%
Fe (mg/L)	1.5	0.03	0.95	0.22	0.198	0	0%
As (ppb)	10	0.13	79.65	16.5	22.276	19	28%
Turbidity (NTU)	<5	0.01	15.61	1.15	2.681	2	2%

Note: E.P.L: Exceeding Permissible Limit.

4.2. Arsenic Occurrence and Distribution

The concentration of arsenic in water samples varied widely from 0.13 to 79.65 ppb, with a median value of 16.5. About 28% of the water samples showed arsenic levels higher than the specified limitation of WHO 10 µg/L, demonstrating that arsenic in the research area is an alarming situation for human health and natural habitats. Kouzul noted that continuous water consumption with arsenic, even 3 µg/L, can cause serious health issues, such as cancer in the human body [54].

The spatial distribution map was constructed through the interpolation method in Arc GIS to present the spatial distribution of arsenic contamination in the research area (Figure 2). For representing the spatial distribution of elements in groundwater, the inverse distance weighting (IDW) technique is regarded to be a better interpolation technique [55]. The IDW technique is simple and requires minimal inputs for interpolation. IDW interpolation was performed on the dataset utilizing its powers 1–4, as well as the ideal power. It employs a weighted reciprocal of distance from the position where the value is to be acquired to previously known points, by arranging values in a linear way [56]. It is predicated on the premise that a sampled point that is closer to an unsampled point has a greater similarity to that unsampled point than the value of a sampled point [57]. In the current study, high arsenic was recorded in the certain areas of Nankana District, such as Syed Wala, Mandi Faizabad, More Khunda, Rehan Wala, and Khiary Kalan. These areas are located near River Ravi. In Pakistan, the most important aquifer exists in the Indus Plain. Quaternary sedimentary deposits dominate the Indus Plain, mostly of glacial and alluvial origin. The sedimentary aquifer of the Indus Plain of this part has higher concentrations of arsenic [58].
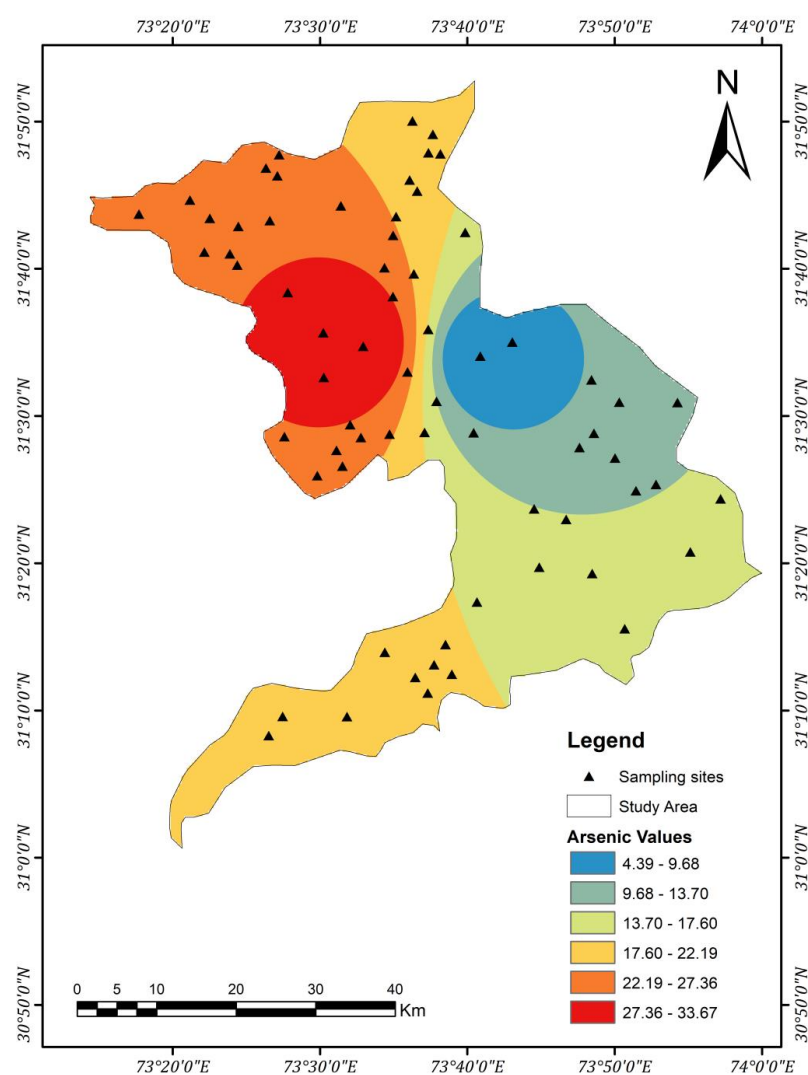

Figure 2. Map of the spatial distribution of arsenic in the research area.

Various scatter plots were plotted to explain the correlation between arsenic and other chemical elements in groundwater samples. The scatter plot (Figure 3a–c) depicted high arsenic concentrations in the pH values between 7.4 and to 7.94. Arsenite (V) and

arsenate (III) in groundwater are primarily is the form of oxyanions, so their adhesion to such surfaces decreases when increased pH results in arsenic mobilization [59]. Arsenic can be mobilized in groundwater by the influence of HCO_3^- ions through carbonization of As-bearing sulfide minerals [60,61]; however, in our study, HCO_3^- showed a weak correlation with arsenic, suggesting no influence of bicarbonate in the mobilization of arsenic in groundwater.
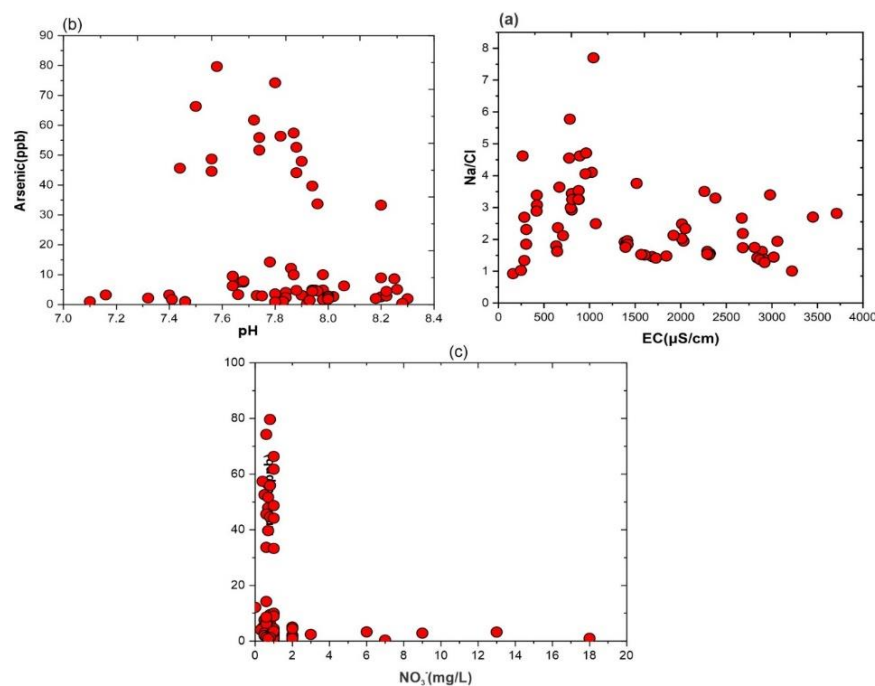

Figure 3. Scatter plot, Na/Cl vs. EC (**a**), scatter plot of As vs. PH (**b**), and NO_3^- vs. As plot (**c**).

Similarly, NO_3^- and SO_4^- depicted a weak correlation with arsenic. The weak correlation of arsenic with NO_3^- and SO_4^- often indicates a strongly reducing environment, which probably increases the arsenic in the groundwater [62]. Moreover, As and Fe did not show a positive correlation in Figure 4b. According to previous research [63–67], the minimum correlation between As and Fe might be due to the reduction of Fe-oxyhydroxides combined with the precipitation of Fe^{2+} as $FeCO_3$ when an anaerobic environment prevails during bacterial oxidation of sedimentary organic matter. Furthermore, scatter plots of phosphate and sulfate vs. arsenic depicted a weak correlation of phosphate and sulfate with arsenic, indicating no significant role of these ions in the movement of arsenic.

4.2.1. Groundwater Type

The piper diagram was used to understand the hydrochemical evolution and the impact of significant ion processes in the groundwater of the study area [68]. In the piper diagram, water samples are generally divided into six major categories: (i) Ca-HCO_3^- type, (ii) Na-Cl type, (iii) Ca–Mg–Cl type, (iv) Ca-Na-HCO_3^- type, (v) Ca–Cl type, and (vi) Na-HCO_3^- type [69]. The piper diagram (Figure 5) reflects three prominent water types in the study: calcium type, chloride type, and calcium chloride type, whereas water of sulfate type, mixed CaMgCl type and no dominant type was also found in the area. The diagram indicates that calcium and chloride are the principal cation and anion, respectively. The most probable sources of calcium in groundwater are the dissolution of carbonate rocks by carbonic acid. Human activities might also impart the enhancement of calcium in the groundwater by using lime as an agricultural fertilizer [70,71].
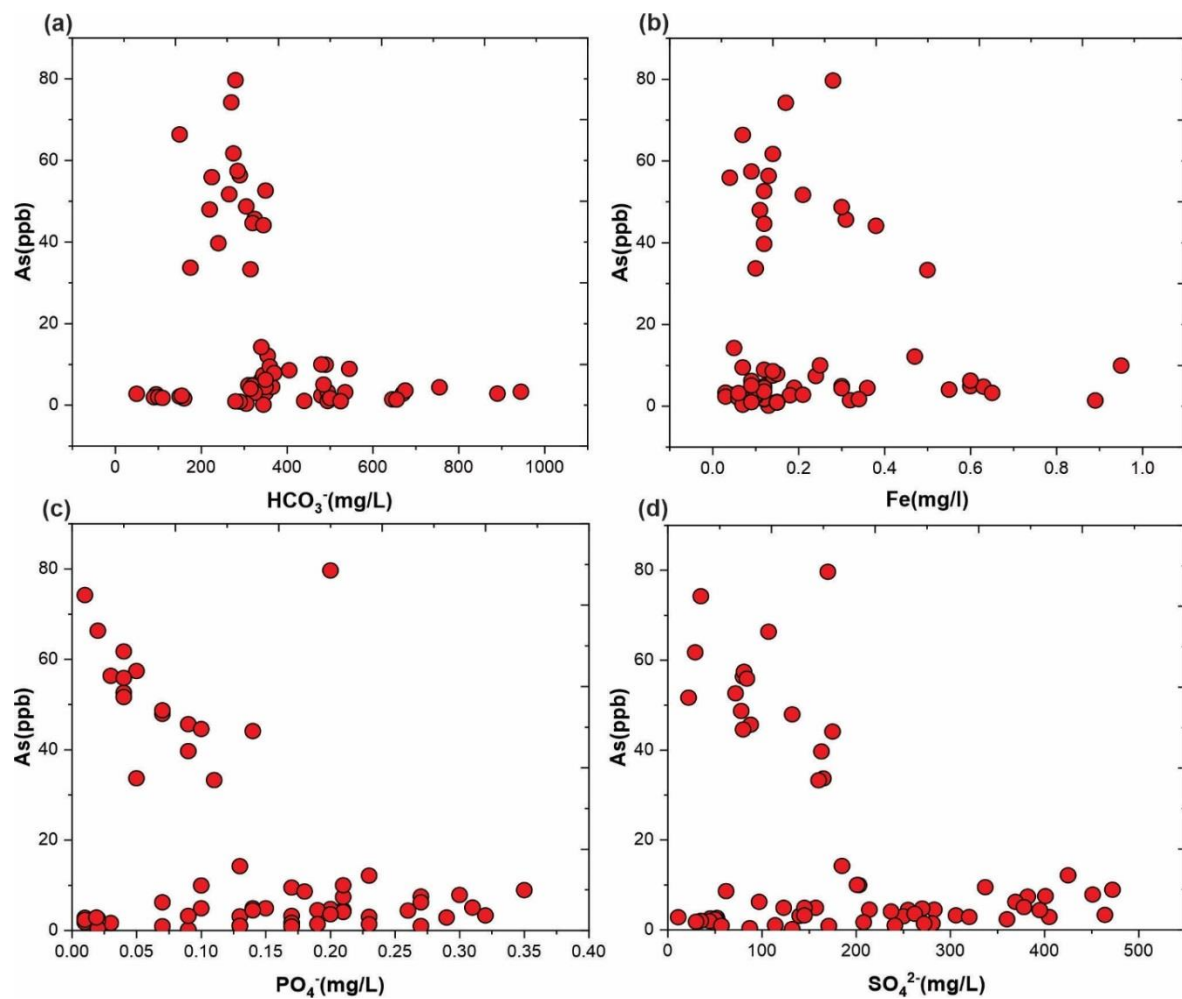
Figure 4. (**a–d**) Relationship between arsenic and other chemical parameters in the research area.

4.2.2. Groundwater Chemistry Controlling Mechanisms

Precipitation, evaporation, and rock–water interaction are prominent hydrogeochemical processes in semi-arid areas, and these processes mainly govern the water chemistry of these regions [72]. The Gibbs plot explains the mechanisms of groundwater of the study area. The two semi-logarithm diagrams showed the precipitation dominance. Chloride contamination in groundwater could be caused by either natural or anthropogenic sources, such as weathering of chloride-bearing rocks, evaporation, intrusion of seawater, leakage of industrial or domestic waste rock dominance, and evaporation dominance [73]. In the Gibbs plot, the ratios of significant cations [(Na + K)]/(Na + KCa)] and anions [(Cl/Cl + HCO_3)] were plotted individually against TDS (Figure 6). The plot demonstrates that many water samples fall in the rock-dominance zone. These findings imply that the process of rock and mineral weathering is the most significant factor influencing groundwater quality in the research area. Some samples in the cation section fall beyond the plot preview, indicating anthropogenic contamination [74]. Furthermore, several bivariate plots are also constructed to better comprehend the weathering mechanisms of the rock-water interaction processes [75,76].
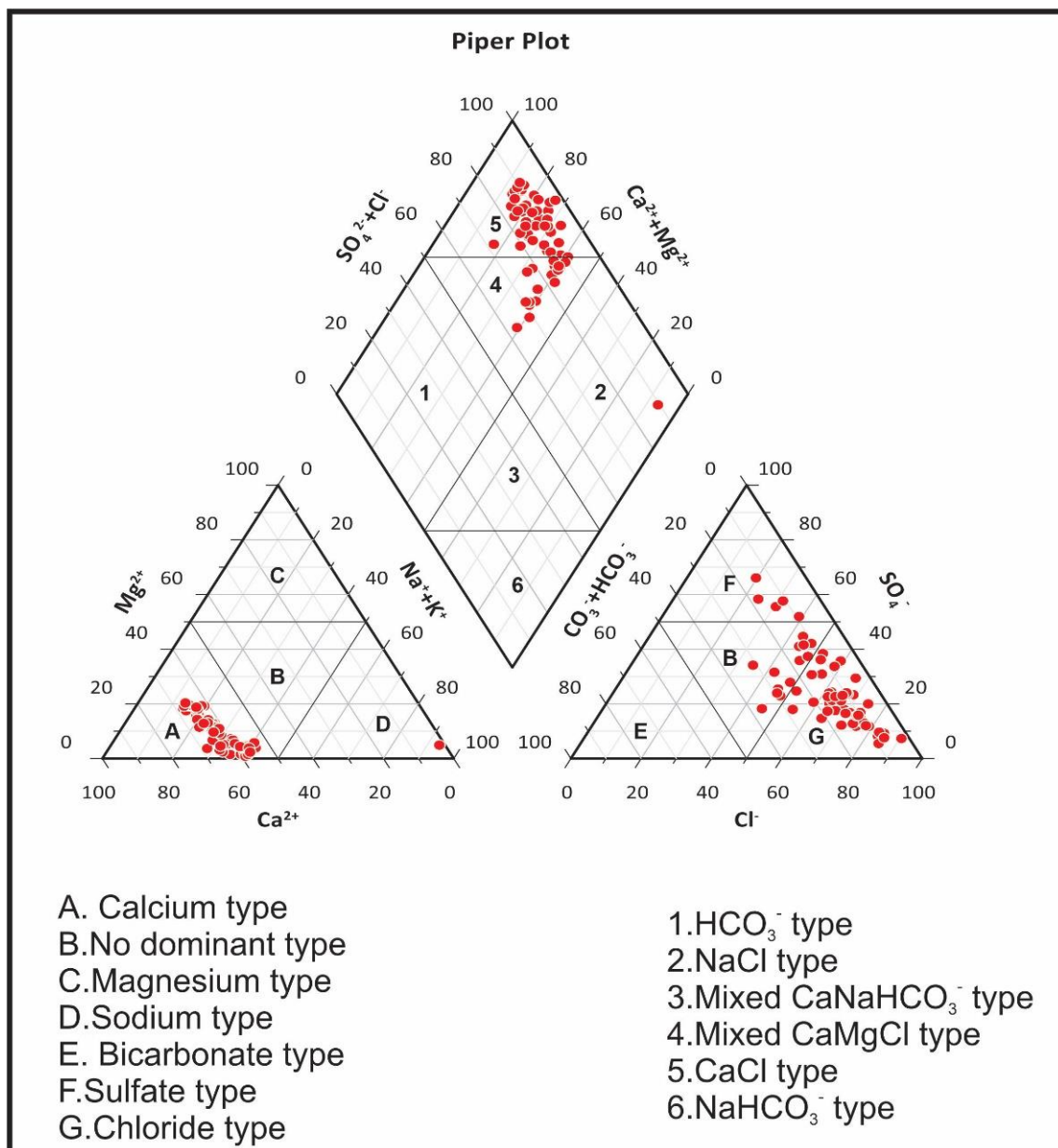
Figure 5. Piper diagram of groundwater samples from the study area.

(1)   Silicate Weathering

Silicate weathering considers the primary geochemical process influencing the hydrochemistry of significant ions, particularly in aquifers of hard rocks [77]. The concentrations because of silicate weathering could be evaluated by the bivariate plot of $Ca^+ + Mg^+/TZ^+$ (7d). The scatter plot (Figure 7d) shows that most samples fall above and towards the $Ca^{2+} + Mg^{2+} = 0.5$ line, indicating the predominant role of silicate weathering in geochemical processes. In contrast, some samples lie below the $Ca^{2+} + Mg^{2+} = 0.5$ line, which indicates that the abundance of $Ca^{2+} + Mg^{2+}$ is probably due to the contribution of reverse ions exchange and weathering of carbonate minerals [78,79].

Figure 6. Gibbs plot depicting the composition of ions in the groundwater samples.

Figure 7. Scatter plot of Ca vs. SO_4^{2-} (**a**), plot of Ca Vs HCO_3^- (**b**), plot of $HCO_3^- + SO_4^{2-}$ vs. Ca + Mg plot (**c**), and scatter plot of Ca + Mg/TZ^+ (**d**).

(2) Carbonate Weathering and Dissolution

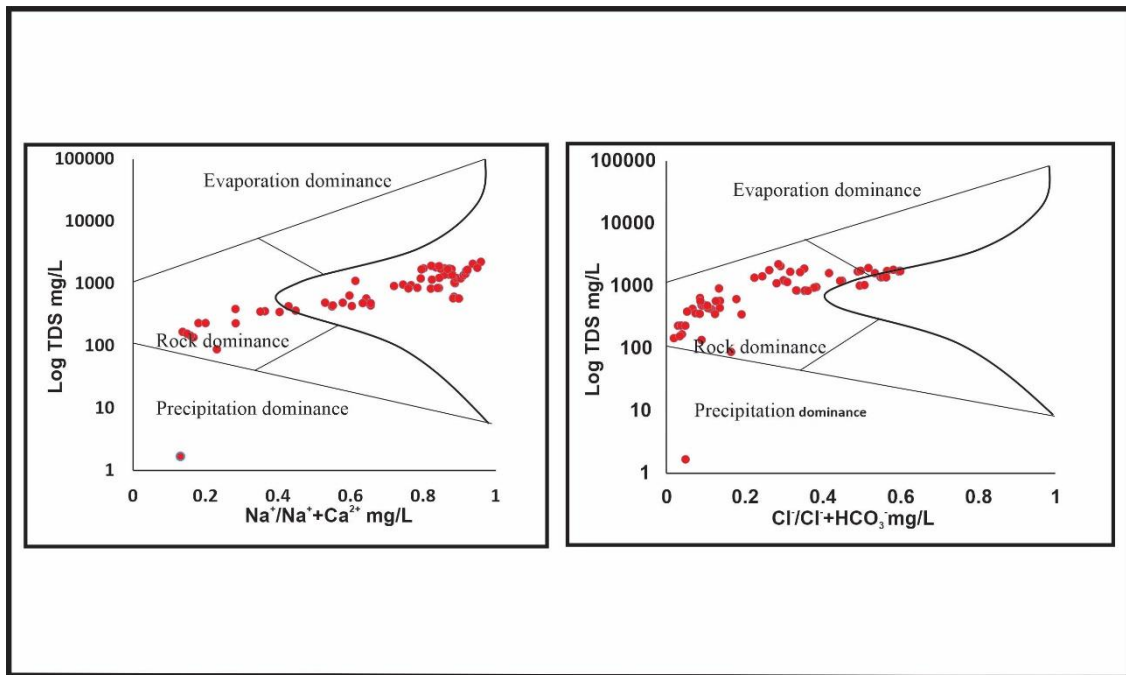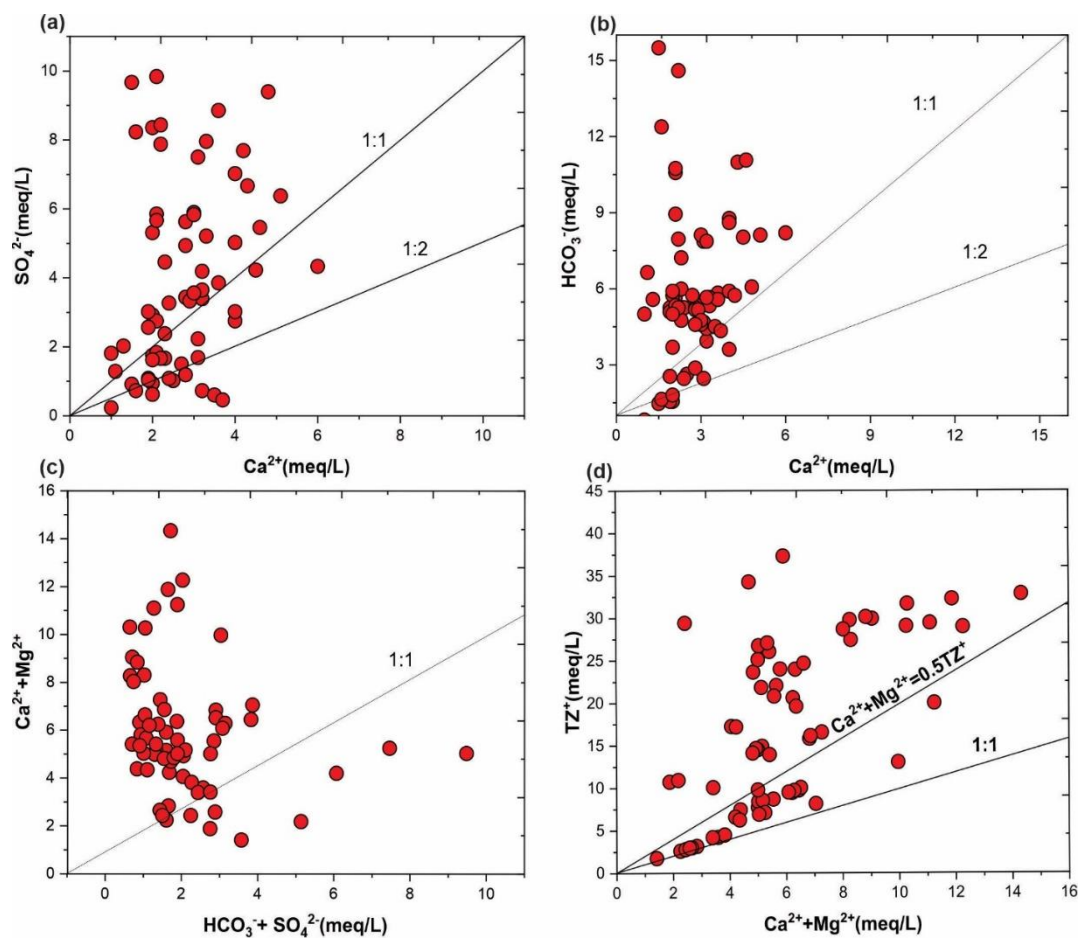The scatter plots of $HCO_3^- + SO_4^{2-}/Ca^{2+} + Mg^{2+}$ and Ca^{2+}/HCO_3^- were used to analyze the carbonate weathering in the research area. Figure 7c depicts the prevalence of bicarbonate over calcium. According to Das et al., if the ratio between bicarbonate and calcium is close to 1:2, the line suggests silicate weathering, while a ratio close to 1:4 indicates carbonate weathering [78]. As plot 7c shows, most samples fall beside the 1:4 line, demonstrating carbonate weathering in our study area. In the $HCO_3^- + SO_4^{2-}$ vs. $Ca^{2+} + Mg^{2+}$ plot (Figure 7c), many samples lie above the 1:1 line, implying the predominance of carbonate weathering, and samples that fall below the line suggest silicate weathering [80,81]. Furthermore, the Ca^{2+} vs. SO_4^{2-} scatter plot (Figure 7a) shows the dominance of sulfate over calcium. Samples falling above the 1:1 line imply the dissolution of gypsum or anhydrite, whereas the fall on the 1:2 lines suggests carbonate weathering. [80].

(3) Evaporation

The evaporation process could be predicted by illustrating the Na/Cl vs. EC plot. No mineral species are expected to precipitate if the dominant controlling process is evaporation; hence, the Na/Cl ratio remains constant. If the ratio of sodium and chloride increases with electrical conductivity (EC), it reveals a predominance of silicate weathering. [50]. The Na/Cl vs. EC plot of our study area illustrates that the Na/Cl ratio is inversely proportional to EC, while some samples are positively correlated with EC. If Na/Cl increases with EC, the predominant mechanism is silicate weathering, whereas decreasing this ratio would promote salt dissolution [50,78].

5. Multivariate Statistical Analysis

5.1. Pearson's Correlation Analysis

Table 2 illustrates the calculated Pearson's correlation matrix. The estimated matrix revealed that EC and TDS have a positive correlation with HCO_3^-, Cl^-, SO_4^-, Na^+ and PO_4^-, showing that these dissolve ions strongly influence TDS and EC values [82]. This implies that the sources of these ions in groundwater are probably fluid-rock interaction and/or anthropogenic practices, such as agricultural activities and sewage from the household [83]. Furthermore, a positive correlation between Na^+ and Cl^- (r = 0.88) reflects that the source of both sodium and chloride in groundwater might be the weathering of halite. Similarly, Ca^{2+} and Mg^{2+} are positively correlated with total hardness = 0.75 and r = 0.95, respectively. The positive correlation is because hardness is the estimated measure of calcium and magnesium [84–86].

The present study explains the insignificant correlation between various chemical parameters and arsenic in groundwater. It suggests that Pearson's correlation matrix could not relate As level to different geochemical variables. As a result, the physicochemical parameters and As were processed for PCA to observe any correlations among the possible As sources in the aquifers.

5.2. Principal Component Analysis

This analysis has become an extensively employed multivariate analytical approach that reduces a range of original variables, such as geochemical data, to a minimal figure of indices (i.e., principal components or factors) for interpreting variations between observed data that are not observable from the simple correlation analysis [23].

A PCA was used to identify differences among the physicochemical variables and evaluate potential hydrogeochemical factors that cause arsenic enrichment in groundwater. The results of five principal components, PC1-PC5, are presented in Table 3 and (Figure 8a–d). The screen plot depicts that three component factors have an eigenvalue greater than 1 (Figure 8). The principal component of PC1, contributing approximately 49.32% of the total variance, showed positive results with EC, HCO_3, Cl, SO_4, Mg, hardness, Na, and PO_4 (Table 3). The result of PCA1 predicted that the main cations and anions were

obtained by rock–water interaction and mineral weathering, such as silicate, carbonate, or evaporation [87,88]. Similarly, in PC2, positive loading was attributed to Ca, Mg, hardness, NO_3, and Fe, whereas PCA_3 showed 8.55% total variance with positive loading on Ca, K, NO_3, Fe, and As. PCA_4 explained the 5.65% total variance with positive loading on As, HCO_3, and Fe, while PCA_5 accounted for 4.90% of the total variance, showing a positive correlation with HCO_3, NO_3, Fe, and F. The positive correlation of NO_3 specifies that the source of nitrate concentration is possibly anthropogenic.

Table 2. Chemical composition of groundwater in the research area as determined using Pearson's correlation matrix.

Parameters	EC	pH	Turbidity	TDS	Alkalinity	HCO_3^-	Cl^-	SO_4^{2-}	Ca^{2+}	Mg^{2+}	Hardness	Na^+	K^+	NO_3^-	PO_4^-	F^-	Fe	As
EC	1																	
pH	−0.18	1																
Turbidity	0.21	0.12	1															
TDS	**0.95**	−0.18	0.20	1														
Alkalinity	**0.76**	−0.14	0.17	**0.79**	1													
HCO_3^-	**0.76**	−0.14	0.17	**0.79**	**1.00**	1												
Cl^-	**0.86**	−0.21	0.12	**0.92**	0.52	0.52	1											
SO_4^{2-}	**0.88**	−0.08	0.28	**0.94**	0.69	**0.69**	**0.85**	1										
Ca^{2+}	0.34	−0.56	−0.01	0.36	0.19	0.19	0.40	0.29	1									
Mg^{2+}	0.53	−0.58	0.01	0.61	0.47	0.47	0.61	0.48	0.48	1								
Hardness	0.54	−0.65	0.00	0.60	0.42	0.42	**0.62**	0.49	**0.75**	**0.94**	1							
Na^+	**0.93**	−0.01	0.21	**0.97**	**0.78**	**0.78**	**0.88**	**0.94**	0.19	0.43	0.40	1						
K^+	0.45	−0.27	0.10	0.53	0.48	0.48	0.50	0.38	0.22	0.55	0.49	0.44	1					
NO_3^-	0.34	−0.41	−0.09	0.36	0.33	0.33	0.34	0.19	0.25	0.54	0.49	0.23	0.56	1				
PO_4^-	**0.86**	−0.09	0.25	**0.81**	0.64	**0.64**	**0.73**	**0.82**	0.17	0.38	0.36	**0.83**	0.41	0.12	1			
F^-	0.46	0.26	−0.02	0.48	0.61	**0.61**	0.29	0.49	−0.13	0.06	−0.01	0.56	0.14	0.13	0.52	1		
Fe	0.28	−0.06	0.10	0.25	0.15	0.15	0.29	0.20	0.22	0.00	0.09	0.28	−0.11	−0.01	0.24	0.08	1	
As	−0.38	−0.17	0.01	−0.41	−0.26	−0.27	−0.43	−0.35	0.10	−0.19	−0.10	−0.44	−0.25	−0.19	−0.31	−0.27	−0.08	1

Table 3. PCA for arsenic along with other chemical variables present in the groundwater of the study area.

| Variable	PC1	PC2	PC3	PC4	PC5
EC (µS/cm)	**0.33**	0.10	0.09	0.03	−0.04
pH	−0.11	**0.47**	−0.09	−0.12	−0.12
TDS (mg/L)	**0.35**	0.08	0.04	0.00	−0.06
HCO_3 (mg/L)	**0.28**	0.11	−0.11	**0.33**	**0.25**
Cl (mg/L)	**0.32**	0.02	0.10	−0.23	−0.19
SO_4 (mg/L)	**0.32**	0.15	0.11	0.08	**−0.22**
Ca (mg/L)	0.15	**−0.37**	**0.35**	0.06	−0.04
Mg (mg/L)	**0.25**	**−0.33**	−0.13	−0.03	−0.10
Hardness (mg/L)	**0.25**	**−0.39**	0.05	0.00	−0.11
Na (mg/L)	**0.33**	0.21	0.06	0.00	−0.06
K (mg/L)	0.21	−0.14	**−0.43**	−0.03	0.03
NO_3 (N)(mg/L)	0.16	**−0.26**	**−0.41**	−0.14	**0.53**
PO_4 (mg/L)	**0.29**	0.19	0.10	0.13	−0.11
F (mg/L)	0.17	**0.34**	−0.15	0.36	**0.37**
Fe (mg/L)	0.09	0.07	**0.59**	**−0.35**	**0.61**
As (PPb)	−0.15	−0.19	**0.26**	**0.72**	0.07
Eigenvalue	7.89	2.75	1.36	0.90	0.78
% variance	49.32%	17.24%	8.55%	5.65%	4.90%
Cumulative	49.32%	66.56%	75.11%	80.75%	85.65%
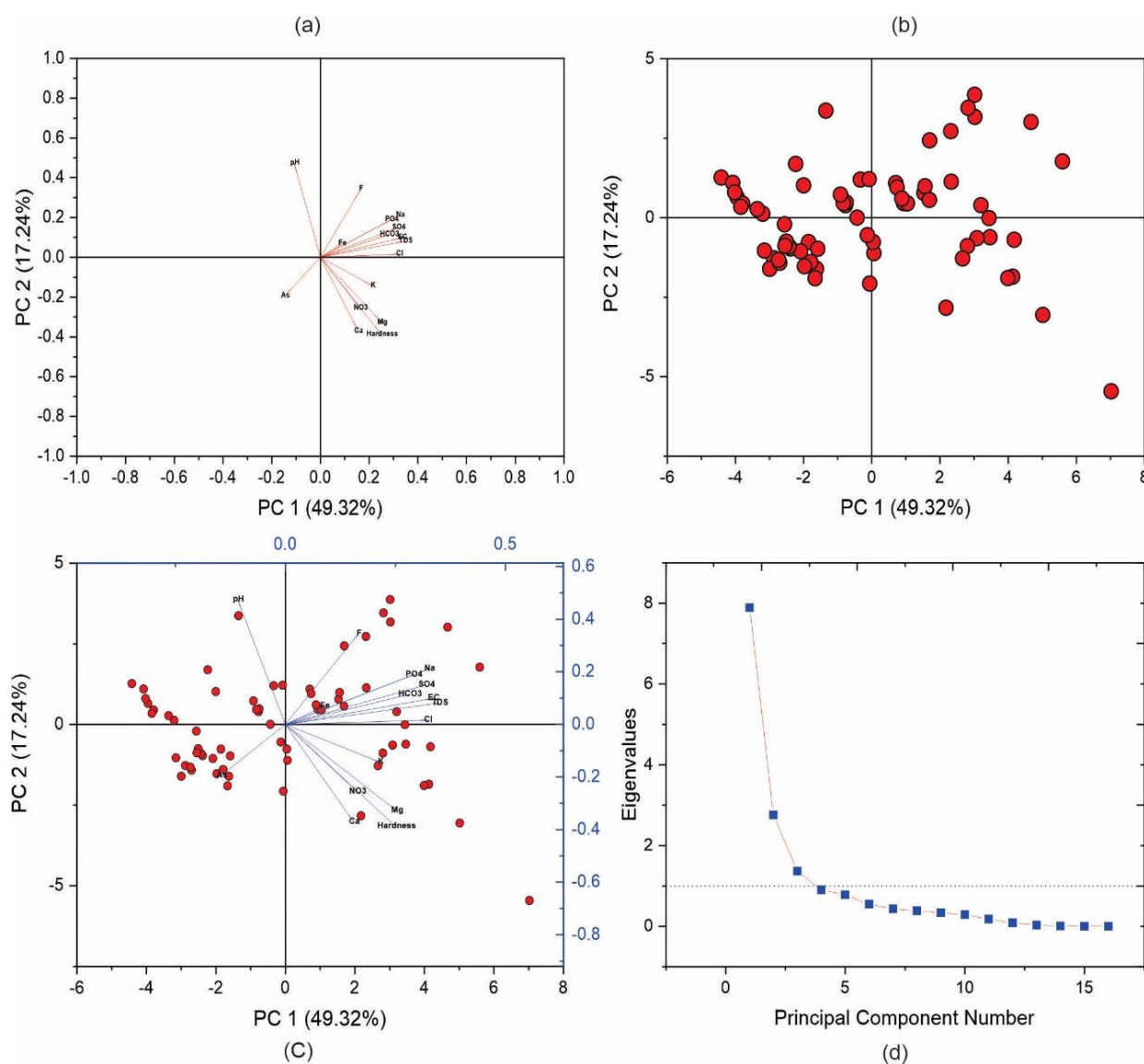
Figure 8. Figure 8 (**a**–**d**) presents the result of PCA.

The score plot, loading plot, and biplot illustrated that pH and As were clustered in one group, whereas all other parameters were assembled on the right side. This suggests that the variables clustered with arsenic play a prominent role in carrying arsenic in groundwater [23]. According to this phenomenon, pH is probably the potential factor controlling arsenic mobilization in the groundwater of our research area.

5.3. Hierarchical Cluster Analysis (HCA)

In hydrogeology, HCA is a broadly utilized cluster analytical technique. It can determine the initial correlation between water samples. It usually employs a dendrogram to depict the relationship graphically [89,90]. The Euclidean distance was used to identify different groundwater samples utilizing hierarchical cluster analysis. The result of cluster analysis was then plotted in the dendrogram (Figure 9a,b). The dendrogram classified the geochemical parameters into two major clusters, i.e., Cluster 1 (sample 1–62) and Cluster 2 (sample 20–67) (Figure 9a). Cluster 2 contained water samples with high arsenic contamination, whereas Cluster 1 included water samples having less arsenic pollution. Clusters of similar properties and correlations were connected at low linkage distances, whereas dissimilar samples showed high linkage distances [91]. Figure 10b classified chemical parameters into three groups. The first group represented EC, TDS, Na, SO$_4$, HCO$_3$, and F.

This group suggests fluid–rock interaction or mineral dissolution [39,76] and these variables also showed the same result in PCA1 (Table 3).
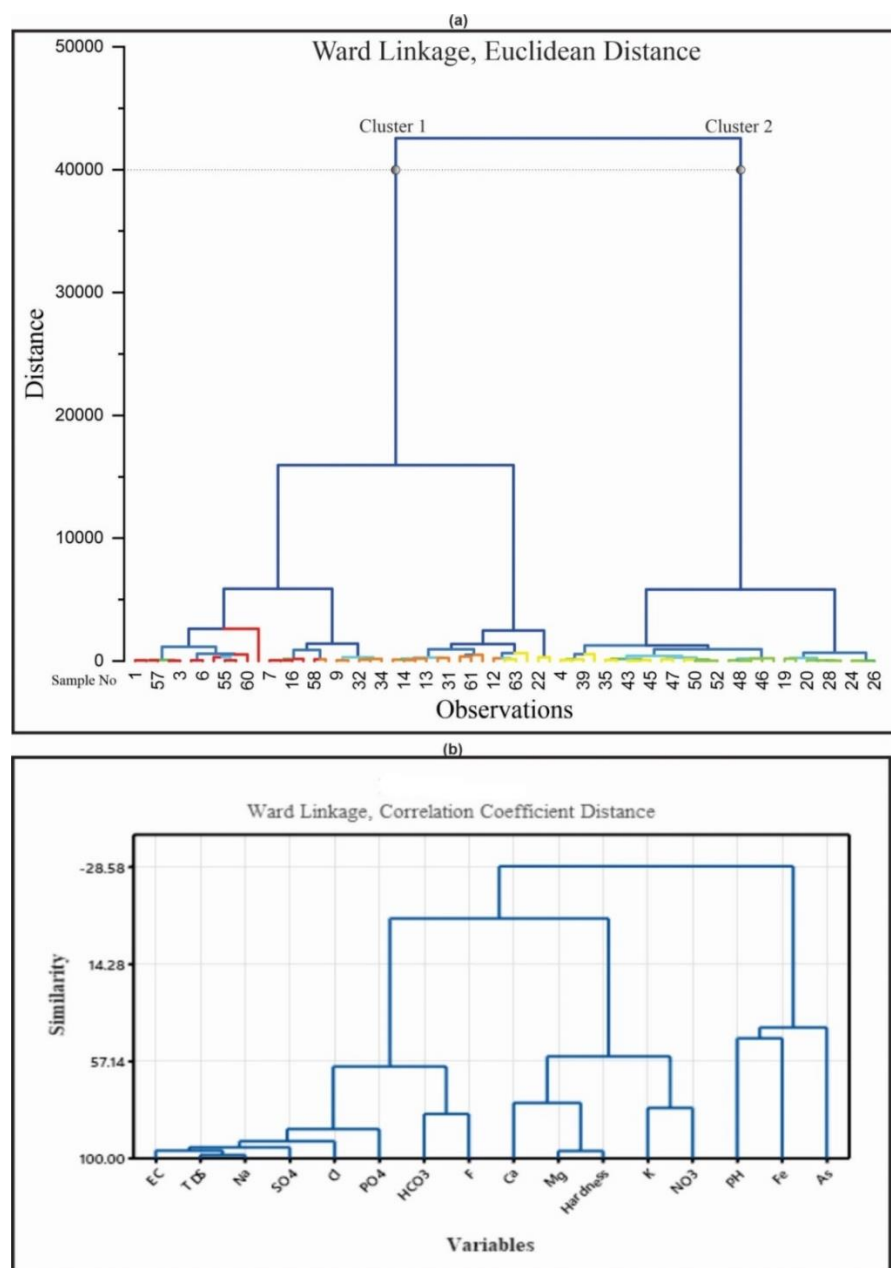

Figure 9. Dendrogram classifying hydrochemical parameters into clusters based on their chemical characteristics.

Furthermore, the second group showed close similarities between Ca, Mg, hardness, K, and NO_3, while the third group illustrated the close correlation of As, Fe, and pH. In the As vs. Fe scatter plot (7b), some samples showed a positive correlation between As and Fe. Hence, the results of cluster analysis in the dendrogram (9b) also validate the observation of the predominant reducing environment in the aquifer, which accelerates arsenic extraction from Fe oxides into the groundwater.
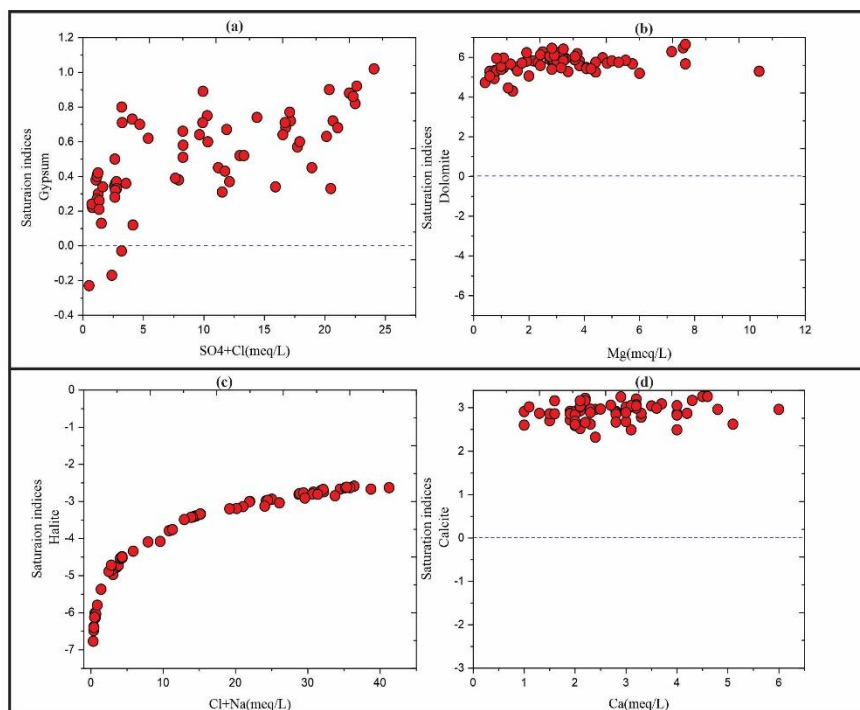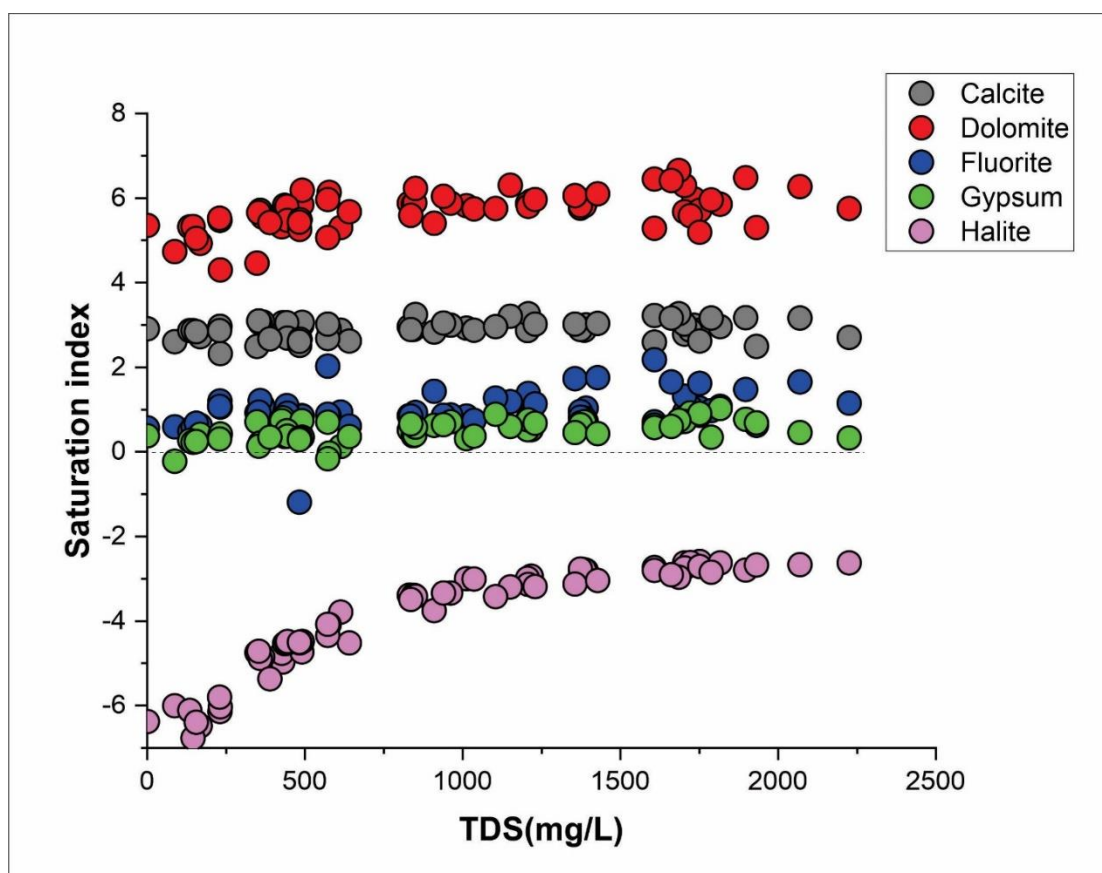
Figure 10. (**1**) Mineral saturation indices in groundwater samples with TDS. (**2**) Saturation index scatter plot of calcite, dolomite, halite and gypsum (**a–d**).

6. Geochemical Modeling

6.1. Mineral Saturation Index

Saturation indices (SI) are useful for determining mineral reactivity in groundwater. The SI was computed by utilizing the equation below:

$$SI = \log \left(\frac{IAP}{Ks(T)} \right) \tag{10}$$

In Equation (10), IAP represents the ionic activity product and K signifies the equilibrium constant. Positive SI values specify mineral oversaturation, which leads to precipitation, while negative SI values specify mineral unsaturation, which results in mineral dissolution. Saturation indices were computed and are presented in (Figure 10a,1). The scatter plot (Figure 10b,d) of calcite vs. Ca and dolomite vs. Mg illustrate positive SI values for calcite and dolomite, suggesting that the minerals are oversaturated in the preponderance of the samples. The study area has a semi-arid climatic condition. According to [92], due to low rainfall, the precipitation of calcite and dolomite occurs in the groundwater of semi-arid regions. The saturation indices of halite showed a negative value where all the samples fell below the 0 lines, implying the dissolution of halite mineral in the groundwater samples (Figure 10c). The scatter plot of gypsum vs. SO_4 + Cl shows that only a few samples fell below the 0 lines, suggesting that gypsum dissolution is not a predominant process affecting the groundwater chemistry of the research area.

6.2. Ion Exchange

The chloro-alkaline index (CAI) measures the amount of ion exchange amongst aquifer minerals and groundwater. An ion-exchange mechanism in groundwater can be evaluated using this method. Whenever the direct ion exchange process occurs, chloro-alkaline exhibits a negative value. During the direct ion exchange process, K^+ and Na^+ are released from the aquifer and exchanged with trapped Mg and Ca in groundwater. Low salinity and freshwater often show a negative chloro-alkaline value [93]. Positive chloro-alkaline indices explain the reverse ion exchange process, where Ca^{2+} and Mg^{2+} are released from the aquifer and exchanged with K^+ and Na^+ trapped in groundwater. Reverse ion exchange could result from the intrusion of seawater and sewage water into the aquifer [94].

In the current study, the CAI-I and CAI-II values extended from −6.83 to 14.89, exhibiting an average of 2.90, and −0.09 to 14.71 showing an average of 4.74, respectively. The chloro-alkaline index results revealed that direct and reverse ion exchange processes were involved in controlling groundwater chemistry in this area.

7. Health Risk Assessment

The health risk assessment ingestion was performed for the District Nankana Sahib. Table 4 presents the assessment result concerning the average daily dosage, hazard quotient, and cancer risk assessment for individuals consuming arsenic-rich contaminated groundwater. The computed ADD levels in the study region varied from 0 to 2.28 (μg/kg/day), with a median of 0.47g/μg/day, whereas the values of HQ varied from 0.01 to 7.59, with a mean value of 1.57 μg/kg/day (Figure 11); 28% of the groundwater samples showed a value of HQ greater than 1, exceeding the toxic limit. According to HQ's findings, 28% of the samples are highly hazardous to inhabitants on continued consumption of polluted water. The carcinogenic risk (CR) due to consuming arsenic polluted water varied from 5.57×10^{-3} to 3.41×10^{0}, with an average value of 7.07×10^{-1}, as shown in Table 4. The prescribed limit of CR by USEPA (US Environmental Protection Agency) is 1×10^{-6} (1 chance in 1,000,000 lifetime exposure) to 1×10^{-4} (1 chance in 10,000-lifetime exposure), and unacceptable if the CR value exceeds 1×10^{-4} [95]. These findings demonstrated that drinking arsenic-contaminated water poses a significant health risk to most inhabitants in the research area. As a result, areas exposed to arsenic should take considerable measures to protect inhabitants from arsenic exposure.

Table 4. Average daily intake (mg/kg/day), hazard quotient, and cancer risk assessment results calculated for the groundwater of the research area.

Sample	As (ppb)	ADD	HQ	CR
1	4.9	0.14	0.47	2.1×10^{-1}
2	3.1	0.09	0.30	1.32×10^{-1}
3	0.13	0.00	0.01	5.57×10^{-3}
4	6.21	0.18	0.59	2.66×10^{-1}
5	4.91	0.14	0.47	2.10×10^{-1}
6	4.91	0.14	0.47	2.10×10^{-1}
7	4.5	0.13	0.43	1.92×10^{-1}
8	4.76	0.14	0.45	2.0×10^{-1}
9	4.49	0.13	0.43	1.92×10^{-1}
10	4.45	0.13	0.42	1.90×10^{-1}
11	12.1	0.35	1.15	5.2×10^{-1}
12	7.51	0.21	0.72	3.21×10^{-1}
13	7.38	0.21	0.70	3.16×10^{-1}
14	9.48	0.27	0.90	4.06×10^{-1}
15	3.01	0.09	0.29	1.29×10^{-1}
16	4.06	0.12	0.39	1.74×10^{-1}
17	7.86	0.22	0.75	3.33×10^{-1}
18	6.22	0.18	0.59	2.66×10^{-1}
19	2.57	0.07	0.24	1.11×10^{-1}
20	2.67	0.08	0.25	1.11×10^{-1}
21	2.81	0.08	0.27	1.20×10^{-1}
22	2.87	0.08	0.27	1.23×10^{-1}
23	3.3	0.09	0.31	1.41×10^{-1}
24	1.65	0.05	0.16	7.07×10^{-2}
25	2.12	0.06	0.20	9.08×10^{-2}
26	2.35	0.07	0.22	1.07×10^{-1}
27	1.94	0.06	0.18	8.31×10^{-2}
28	1.98	0.06	0.19	8.48×10^{-2}
29	1.78	0.05	0.17	7.62×10^{-2}
30	2.36	0.07	0.22	1.01×10^{-1}
31	3.23	0.09	0.31	1.38×10^{-1}
32	9.94	0.28	0.95	4.26×10^{-1}
33	1.03	0.03	0.10	4.41×10^{-2}
34	9.96	0.28	0.95	4.26×10^{-1}
35	47.94	1.37	4.57	2.05×10^{0}
36	33.68	0.96	3.21	1.44×10^{0}
37	39.67	1.13	3.78	1.7×10^{0}
38	1.03	0.03	0.10	4.0×10^{-2}
39	0.36	0.01	0.03	1.54×10^{-2}
40	3.21	0.09	0.31	1.37×10^{-2}
41	74.23	2.12	7.07	3.18×10^{0}
42	52.59	1.50	5.01	2.25×10^{0}
43	56.31	1.61	5.36	2.41×10^{0}
44	57.41	1.64	5.47	2.46×10^{0}
45	55.87	1.60	5.32	2.39×10^{0}
46	66.34	1.90	6.32	2.84×10^{0}
47	79.65	2.28	7.59	3.41×10^{0}
48	61.73	1.76	5.88	2.56×10^{0}
49	51.66	1.48	4.92	2.21×10^{0}
50	45.62	1.30	4.34	1.96×10^{0}
51	44.59	1.27	4.25	1.96×10^{0}
52	48.67	1.39	4.64	2.09×10^{0}
53	2.84	0.08	0.27	1.21×10^{-1}
54	3.59	0.10	0.34	1.53×10^{-1}

Table 4. *Cont.*

Sample	As (ppb)	ADD	HQ	CR
55	14.2	0.41	1.35	6.08×10^{-1}
56	44.12	1.26	4.20	1.89×10^{0}
57	33.28	0.95	3.17	1.43×10^{0}
58	1.43	0.04	0.14	6.12×10^{-2}
59	1.35	0.04	0.13	5.78×10^{-2}
60	1.69	0.05	0.16	7.24×10^{-2}
61	0.97	0.03	0.09	4.15×10^{-2}
62	5.04	0.14	0.48	2.16×10^{-1}
63	8.93	0.26	0.85	3.82×10^{-1}
64	8.59	0.25	0.82	3.68×10^{-1}
65	0.86	0.02	0.08	3.68×10^{-2}
66	4.39	0.13	0.42	1.88×10^{-1}
67	0.9	0.03	0.09	3.85×10^{-2}
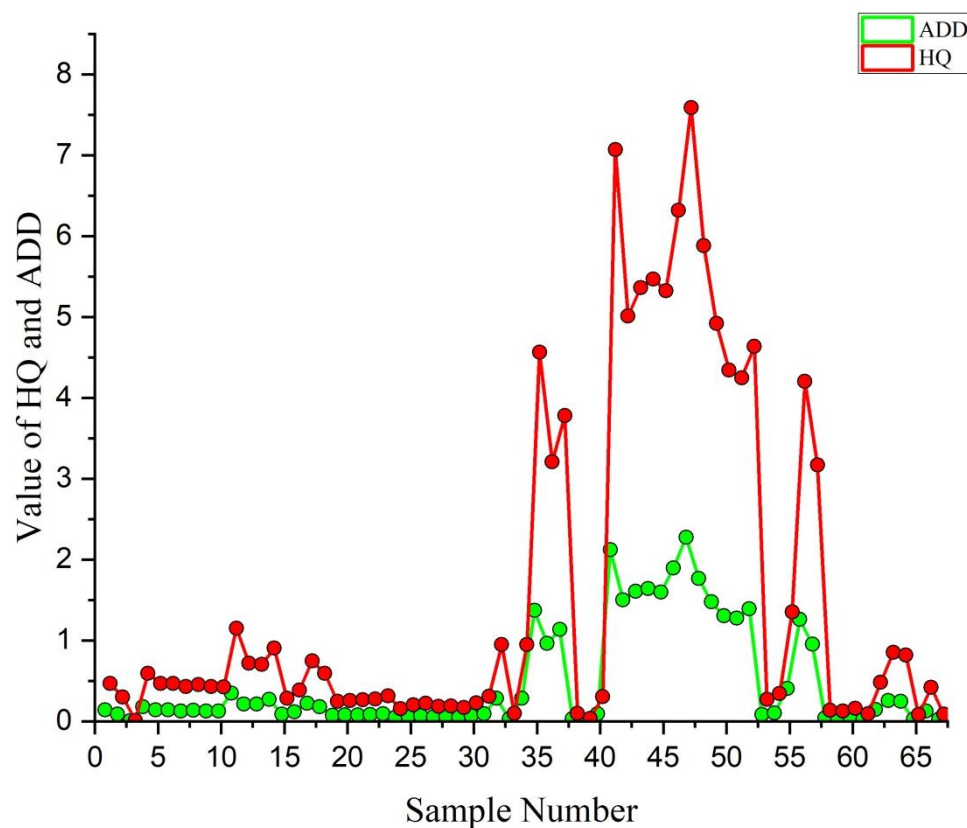
Figure 11. Range of ADD and HQ values in groundwater samples.

8. Water Quality Index

The WQI is commonly applied to assess drinking water quality. Using the Brown weighted arithmetic index, the water quality indices were determined. In contrast, the WQI spatial distribution map was constructed by employing the interpolation method in Arc GIS to examine the distribution pattern of water quality in the present research. The WQI value is used to classify water quality into different categories. Water quality is considered excellent if the WQI value is 0–25, good if the WQI value is 26–50, poor if the WQI value is 51–75, very poor if the WQI value is 76–100, and unfit for drinking if the WQI value is >100 [43,96]. Table 5 illustrates the WQI categorization of the research area, including a list of the various types of groundwater based on WQI sources. In contrast, the WQI spatial distribution map is also presented in (Figure 12). The water quality indices indicate

that 19% of groundwater samples were considered excellent for human consumption. In comparison, 32% were good, 22% and 10% were poor and very poor, whereas 11% of the water samples were unsafe for consumption.

Table 5. Classification of water quality based on the WQI.

Category	WQI	Water Quality	Water Sample
A	0–25	Excellent	19%
B	25–50	Good	32%
C	51–75	Poor	22%
D	76–100	Very poor	10%
E	>100	Not suitable	11%
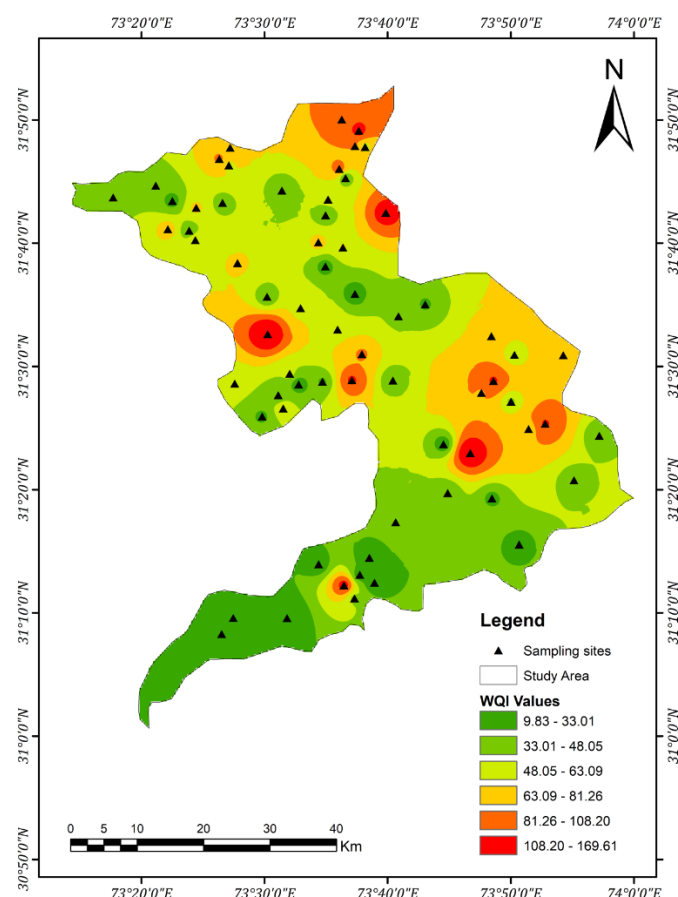
Figure 12. Spatial distribution map of WQI.

9. Conclusions

This study involved the evaluation of the groundwater quality of the District Nankana Sahib according to the concentration of arsenic and its spatial distribution. The pH values stated that the groundwater is well buffered. The water quality index demonstrated that 32% of groundwater samples belong to poor quality, whereas 11% of water samples are unsafe for consumption. Furthermore, the predominant water types in the research area were calcium type, calcium–chloride type, and chloride type, with calcium as the dominant cation and sulfate as the dominant anion. The Gibbs plot indicated that fluid–rock interaction is the most important controlling process influencing the groundwater quality.

Moreover, arsenic levels in 28% of the water samples surpassed the suitable levels provided by WHO guidelines. Stations of Syed Wala, Mandi Faizabad, More Khunda, Rehan Wala, and Khiary Kalan areas reveal maximum arsenic concentration. The correlation

between arsenic and pH was performed because arsenic solubility reduces as pH increases. PCA analysis showed that the correlation between arsenic and other chemical parameters was weak, except for pH, whereas cluster analysis detected a positive correlation between pH, Fe, and As, implying the reducing environment of the aquifer. Moreover, the positive and negative values of chloro-alkaline indices revealed that both direct and reverse ion exchange processes influenced the groundwater chemistry of the research area. The saturation mineral indices indicated the oversaturation of dolomite and calcite, but showed a undersaturation of halite and the dissolution of some gypsum samples. Health risk assessment outcomes exhibited that 28% of the groundwater samples are highly hazardous (HQ) to the residents on lifetime exposure to polluted water.

The present research concluded that due to arsenic contamination and poor groundwater quality, most of the groundwater samples were not appropriate for human consumption without proper treatment and remediation of arsenic. Therefore, it is recommended that proper water quality control monitoring of arsenic contamination be implemented to protect residents from arsenic contamination.

References

1. Barbier, E. A Global Crisis in Water Management. In *The Water Paradox*; Yale University Press: New Haven, CT, USA, 2019; pp. 89–109.
2. Anderson, M.P.; Cherry, J.A. Using models to simulate the movement of contaminants through groundwater flow systems. *Crit. Rev. Environ. Sci. Technol.* **1979**, *9*, 97–156. [CrossRef]
3. Medici, G.; West, L.J. Groundwater flow velocities in karst aquifers; importance of spatial observation scale and hydraulic testing for contaminant transport prediction. *Environ. Sci. Pollut. Res.* **2021**, *28*, 43050–43063. [CrossRef]
4. Mackay, D.M.; Cherry, J.A. Groundwater contamination: Pump-and-treat remediation. *Environ. Sci. Technol.* **1989**, *23*, 630–636. [CrossRef]
5. Bodrud-Doza, M.; Bhuiyan, M.A.H.; Islam, S.D.-U.; Rahman, M.S.; Haque, M.M.; Fatema, K.J.; Ahmed, N.; Rakib, M.; Rahman, M.A. Hydrogeochemical investigation of groundwater in Dhaka City of Bangladesh using GIS and multivariate statistical techniques. *Groundw. Sustain. Dev.* **2019**, *8*, 226–244. [CrossRef]
6. Chen, Y.N.; Ding, L.C.; Liu, C.H. Review of the treatment of water containing arsenic. *Appl. Mech. Mater.* **2013**, *260–261*, 1162–1166. [CrossRef]
7. Tapia, J.; Schneider, B.; Inostroza, M.; Álvarez-Amado, F.; Luque, J.; Aguilera, F.; Parra, S.; Bravo, M. Naturally elevated arsenic in the Altiplano-Puna, Chile and the link to recent (Mio-Pliocene to Quaternary) volcanic activity, high crustal thicknesses, and geological structures. *J. S. Am. Earth Sci.* **2021**, *105*, 102905. [CrossRef]
8. Mukherjee, A.; Bhattacharya, P.; Shi, F.; Fryar, A.E.; Mukherjee, A.B.; Xie, Z.M.; Jacks, G.; Bundschuh, J. Chemical evolution in the high arsenic groundwater of the Huhhot basin (Inner Mongolia, PR China) and its difference from the western Bengal basin (India). *Appl. Geochem.* **2009**, *24*, 1835–1851. [CrossRef]
9. Sohrabi, N.; Kalantari, N.; Amiri, V.; Saha, N.; Berndtsson, R.; Bhattacharya, P.; Ahmad, A. A probabilistic-deterministic analysis of human health risk related to the exposure to potentially toxic elements in groundwater of Urmia coastal aquifer (NW of Iran) with a special focus on arsenic speciation and temporal variation. *Stoch. Environ. Res. Risk Assess.* **2021**, *35*, 1509–1528. [CrossRef]
10. Ahmad, A.; Bhattacharya, P. Arsenic in drinking water: Is 10 µg/L a safe limit? *Curr. Pollut. Rep.* **2019**, *5*, 1–3. [CrossRef]
11. Mandal, B.K.; Suzuki, K.T. Arsenic round the world: A review. *Talanta* **2002**, *58*, 201–235. [CrossRef] [PubMed]

12. Skála, J.; Vácha, R.; Čechmánková, J. Evaluation of arsenic occurrence in agricultural soils of the Bohemian Forest region. *Silva Gabreta* **2011**, *17*, 55–67.

13. Saha, S.; Reza, A.; Roy, M.K. Arsenic geochemistry of the sediments of the shallow aquifer and its correlation with the groundwater, Rangpur, Bangladesh. *Appl. Water Sci.* **2021**, *11*, 166. [CrossRef]

14. Smedley, P.L.; Kinniburgh, D.G. A review of the source, behaviour and distribution of arsenic in natural waters. *Appl. Geochem.* **2002**, *17*, 517–568. [CrossRef]

15. Iqbal, J.; Su, C.; Rashid, A.; Yang, N.; Baloch, M.Y.J.; Talpur, S.A.; Ullah, Z.; Rahman, G.; Rahman, N.U.; Sajjad, M.M. Hydrogeochemical assessment of groundwater and suitability analysis for domestic and agricultural utility in Southern Punjab, Pakistan. *Water* **2021**, *13*, 3589. [CrossRef]

16. Jat Baloch, M.Y.; Zhang, W.; Zhang, D.; Al Shoumik, B.A.; Iqbal, J.; Li, S.; Chai, J.; Farooq, M.A.; Parkash, A. Evolution Mechanism of Arsenic Enrichment in Groundwater and Associated Health Risks in Southern Punjab, Pakistan. *Int. J. Environ. Res. Public Health* **2022**, *19*, 13325. [CrossRef] [PubMed]

17. Shahid, M.; Niazi, N.K.; Dumat, C.; Naidu, R.; Khalid, S.; Rahman, M.M.; Bibi, I. A meta-analysis of the distribution, sources and health risks of arsenic-contaminated groundwater in Pakistan. *Environ. Pollut.* **2018**, *242*, 307–319. [CrossRef]

18. Fatima, S.; Hussain, I.; Rasool, A.; Xiao, T.; Farooqi, A. Comparison of two alluvial aquifers shows the probable role of river sediments on the release of arsenic in the groundwater of district Vehari, Punjab, Pakistan. *Environ. Earth Sci.* **2018**, *77*, 382. [CrossRef]

19. Ullah, Z.; Rashid, A.; Ghani, J.; Talib, M.A.; Shahab, A.; Lun, L. Arsenic Contamination, Water Toxicity, Source Apportionment, and Potential Health Risk in Groundwater of Jhelum Basin, Punjab, Pakistan. *Biol. Trace Elem. Res.* **2022**, *M78*, 1–11. [CrossRef] [PubMed]

20. Memon, M.; Soomro, M.S.; Akhtar, M.S.; Memon, K.S. Drinking water quality assessment in Southern Sindh (Pakistan). *Environ. Monit. Assess.* **2011**, *177*, 39–50. [CrossRef] [PubMed]

21. Mushtaq, N.; Younas, A.; Mashiatullah, A.; Javed, T.; Ahmad, A.; Farooqi, A. Hydrogeochemical and isotopic evaluation of groundwater with elevated arsenic in alkaline aquifers in Eastern Punjab, Pakistan. *Chemosphere* **2018**, *200*, 576–586. [CrossRef] [PubMed]

22. Ullah, Z.; Xu, Y.; Zeng, X.-C.; Rashid, A.; Ali, A.; Iqbal, J.; Almutairi, M.H.; Aleya, L.; Abdel-Daim, M.M.; Shah, M. Non-Carcinogenic Health Risk Evaluation of Elevated Fluoride in Groundwater and Its Suitability Assessment for Drinking Purposes Based on Water Quality Index. *Int. J. Environ. Res. Public Health* **2022**, *19*, 9071. [CrossRef] [PubMed]

23. Shakoor, M.B.; Bibi, I.; Niazi, N.K.; Shahid, M.; Nawaz, M.F.; Farooqi, A.; Naidu, R.; Rahman, M.M.; Murtaza, G.; Lüttge, A. The evaluation of arsenic contamination potential, speciation and hydrogeochemical behaviour in aquifers of Punjab, Pakistan. *Chemosphere* **2018**, *199*, 737–746. [CrossRef] [PubMed]

24. Shabbir, H.; Butt, N.A.; Zafar, A.; Mir, M.K. Role of electrical resistivity method to identify fresh water aquifers in Nankana Sahib, Punjab, Pakistan. *J. Himal. Earth Sci.* **2020**, *53*, 52–59.

25. Nawaz, A.; Farooq, M.; Lal, R.; Rehman, A. Comparison of conventional and conservation rice-wheat systems in Punjab, Pakistan. *Soil Tillage Res.* **2017**, *169*, 35–43. [CrossRef]

26. Ali, A.; Shahbaz, B.; Ashraf, I.; Maqsood, M. A Mixed Method Research to Analyze Fertilizer Sources and Application Methods in Nutrient Stewardship Perspective at Farm Level in Rice-Wheat Cropping Zone of Punjab, Pakistan. *J. Agric. Food* **2022**, *3*, 73–84.

27. Shah, S.H.I.A.; Jianguo, Y.; Jahangir, Z.; Tariq, A.; Aslam, B. Integrated geophysical technique for groundwater salinity delineation, an approach to agriculture sustainability for Nankana Sahib Area, Pakistan. *Geomat. Nat. Hazards Risk* **2022**, *13*, 1043–1064. [CrossRef]

28. Shah, S. Stratigraphy of Pakistan (memoirs of the geological survey of Pakistan). *Geol. Surv. Pak.* **2009**, *M 79*, 22.

29. Aftab, S.M.; Maqsood, T.; Hassan, S.; Hannan, A.; Zaidi, A.R.; Tahir, R. Hypothetical geological model affecting groundwater quality in doabs of Indus Basin, Punjab, Pakistan. *Int. J. Econ. Environ. Geol.* **2018**, *9*, 1–11.

30. Shroder, J. Himalaya to the Sea. In *Geology, Geomorphology and the Quaternary*; Routledge: London, UK, 1993.

31. Akhter, G.; Ge, Y.; Hasan, M.; Shang, Y. Estimation of Hydrogeological Parameters by Using Pumping, Laboratory Data, Surface Resistivity and Thiessen Technique in Lower Bari Doab (Indus Basin), Pakistan. *Appl. Sci.* **2022**, *12*, 3055. [CrossRef]

32. Greenman, D.W.; Bennett, G.D.; Swarzenski, W.V. *Ground-Water Hydrology of the Punjab, West. Pakistan, with Emphasis on Problems Caused by Canal Irrigation*; US Government Printing Office: Washington, DC, USA, 1967; Volume 1.

33. Ghani, J.; Ullah, Z.; Nawab, J.; Iqbal, J.; Waqas, M.; Ali, A.; Almutairi, M.; Peluso, I.; Mohamed, H.; Shah, M. Hydrogeochemical characterization, and suitability assessment of drinking groundwater: Application of geostatistical approach and geographic information system. *Front. Environ. Sci.* **2022**, *10*, 874464. [CrossRef]

34. Ullah, Z.; Rashid, A.; Ghani, J.; Nawab, J.; Zeng, X.-C. Groundwater Contamination through Potentially Harmful Metals and Its Implications in Groundwater Management. *Front. Environ. Sci.* **2022**, *10*, 1021596. [CrossRef]

35. Domenico, P.A.; Schwartz, F.W. *Physical and Chemical Hydrogeology*; Wiley: New York, NY, USA, 1998; Volume 506.

36. Nawab, J.; Rahman, A.; Khan, S.; Ghani, J.; Ullah, Z.; Khan, H.; Waqas, M. Drinking Water Quality Assessment of Government, Non-Government and Self-Based Schemes in the Disaster Affected Areas of Khyber Pakhtunkhwa, Pakistan. *Expo. Health* **2022**, *M 80*, 1–17. [CrossRef]

37. Valder, J.F.; Long, A.J.; Davis, A.D.; Kenner, S.J. Multivariate statistical approach to estimate mixing proportions for unknown end members. *J. Hydrol.* **2012**, *460*, 65–76. [CrossRef]

38. Rashid, A.; Ayub, M.; Khan, S.; Ullah, Z.; Ali, L.; Gao, X.; Li, C.; El-Serehy, H.A.; Kaushik, P.; Rasool, A. Hydrogeochemical assessment of carcinogenic and non-carcinogenic health risks of potentially toxic elements in aquifers of the Hindukush ranges, Pakistan: Insights from groundwater pollution indexing, GIS-based, and multivariate statistical approaches. *Environ. Sci. Pollut. Res.* **2022**, *29*, 75744–75768. [CrossRef] [PubMed]

39. Boonkaewwan, S.; Sonthiphand, P.; Chotpantarat, S. Mechanisms of arsenic contamination associated with hydrochemical characteristics in coastal alluvial aquifers using multivariate statistical technique and hydrogeochemical modeling: A case study in Rayong province, eastern Thailand. *Environ. Geochem. Health* **2021**, *43*, 537–566. [CrossRef] [PubMed]

40. Rashid, A.; Ayub, M.; Javed, A.; Khan, S.; Gao, X.; Li, C.; Ullah, Z.; Sardar, T.; Muhammad, J.; Nazneen, S. Potentially harmful metals, and health risk evaluation in groundwater of Mardan, Pakistan: Application of geostatistical approach and geographic information system. *Geosci. Front.* **2021**, *12*, 101128. [CrossRef]

41. Parkhurst, D.L.; Appelo, C. User's guide to PHREEQC (Version 2): A computer program for speciation, batch-reaction, one-dimensional transport, and inverse geochemical calculations. *Water-Resour. Investig. Rep.* **1999**, *99*, 312.

42. Rashid, A.; Ayub, M.; Ullah, Z.; Ali, A.; Khattak, S.A.; Ali, L.; Gao, X.; Li, C.; Khan, S.; El-Serehy, H.A.; et al. Geochemical Modeling Source Provenance, Public Health Exposure, and Evaluating Potentially Harmful Elements in Groundwater: Statistical and Human Health Risk Assessment (HHRA). *Int. J. Environ. Res. Public Health* **2022**, *19*, 6472. [CrossRef]

43. Brown, R.M.; McClelland, N.I.; Deininger, R.A.; O'Connor, M.F. A water quality index—Crashing the psychological barrier. In *Indicators of Environmental Quality*; Springer: Berlin/Heidelberg, Germany, 1972; pp. 173–182.

44. Abeer, N.; Khan, S.A.; Muhammad, S.; Rasool, A.; Ahmad, I. Health risk assessment and provenance of arsenic and heavy metal in drinking water in Islamabad, Pakistan. *Environ. Technol. Innov.* **2020**, *20*, 101171. [CrossRef]

45. Rehman, F.; Cheema, T.; Azeem, T.; Naseem, A.A.; Khan, I.; Iqbal, N.; Shaheen, A. Groundwater quality and potential health risks caused by arsenic (As) in Bhakkar, Pakistan. *Environ. Earth Sci.* **2020**, *79*, 529. [CrossRef]

46. US-EPA. *Guidelines for Carcinogen Risk Assessment*; Risk Assesment Forum; US-EPA: Washington, DC, USA, 2005.

47. WHO. *Guidelines for Drinking-Water Quality*; World Health Organization: Geneva, Switzerland, 2011; Volume 216, pp. 303–304.

48. Adelekan, B.; Ogunde, O. Quality of water from dug wells and the lagoon in Lagos Nigeria and associated health risks. *Sci. Res. Essays* **2012**, *7*, 1195–1211. [CrossRef]

49. Ghalib, H.B. Groundwater chemistry evaluation for drinking and irrigation utilities in east Wasit province, Central Iraq. *Appl. Water Sci.* **2017**, *7*, 3447–3467. [CrossRef]

50. Kumar, M.; Ramanathan, A.; Rao, M.S.; Kumar, B. Identification and evaluation of hydrogeochemical processes in the groundwater environment of Delhi, India. *Environ. Geol.* **2006**, *50*, 1025–1039. [CrossRef]

51. Roy, A.; Keesari, T.; Mohokar, H.; Sinha, U.K.; Bitra, S. Assessment of groundwater quality in hard rock aquifer of central Telangana state for drinking and agriculture purposes. *Appl. Water Sci.* **2018**, *8*, 124. [CrossRef]

52. Javed, T.; Sarwar, T.; Ullah, I.; Ahmad, S.; Rashid, S. Evaluation of groundwater quality in district Karak Khyber Pakhtunkhwa, Pakistan. *Water Sci.* **2019**, *33*, 1–9. [CrossRef]

53. Khashogji, M.S.; El Maghraby, M.M. Evaluation of groundwater resources for drinking and agricultural purposes, Abar Al Mashi area, south Al Madinah Al Munawarah City, Saudi Arabia. *Arab. J. Geosci.* **2013**, *6*, 3929–3942. [CrossRef]

54. Kozul, C.D.; Hampton, T.H.; Davey, J.C.; Gosse, J.A.; Nomikos, A.P.; Eisenhauer, P.L.; Weiss, D.J.; Thorpe, J.E.; Ihnat, M.A.; Hamilton, J.W. Chronic exposure to arsenic in the drinking water alters the expression of immune response genes in mouse lung. *Environ. Health Perspect.* **2009**, *117*, 1108–1115. [CrossRef]

55. Shahid, S.U.; Iqbal, J.; Hasnain, G. Groundwater quality assessment and its correlation with gastroenteritis using GIS: A case study of Rawal Town, Rawalpindi, Pakistan. *Environ. Monit. Assess.* **2014**, *186*, 7525–7537. [CrossRef] [PubMed]

56. Shahid, S.U.; Iqbal, J. *Groundwater Quality Assessment Using Averaged Water Quality Index: A Case Study of Lahore City, Punjab, Pakistan*; IOP Conference Series: Earth and Environmental Science; IOP Publishing: Bristol, UK, 2016; p. 042031.

57. Adnan, S.; Iqbal, J. Spatial analysis of the groundwater quality in the Peshawar District, Pakistan. *Procedia Eng.* **2014**, *70*, 14–22. [CrossRef]

58. Smedley, P.L. Sources and distribution of arsenic in groundwater and aquifers. In *Arsenic in Groundwater: A World Problem*; International Association of Hydrogeologists Publication: Utrecht, The Netherlands, 2008.

59. Kim, S.-H.; Kim, K.; Ko, K.-S.; Kim, Y.; Lee, K.-S. Co-contamination of arsenic and fluoride in the groundwater of unconsolidated aquifers under reducing environments. *Chemosphere* **2012**, *87*, 851–856. [CrossRef] [PubMed]

60. Kim, M.-J.; Nriagu, J.; Haack, S. Carbonate ions and arsenic dissolution by groundwater. *Environ. Sci. Technol.* **2000**, *34*, 3094–3100. [CrossRef]

61. Chen, X.; Zeng, X.-C.; Kawa, Y.K.; Wu, W.; Zhu, X.; Ullah, Z.; Wang, Y. Microbial reactions and environmental factors affecting the dissolution and release of arsenic in the severely contaminated soils under anaerobic or aerobic conditions. *Ecotoxicol. Environ. Saf.* **2020**, *189*, 109946. [CrossRef] [PubMed]

62. He, X.; Li, P.; Wu, J.; Wei, M.; Ren, X.; Wang, D. Poor groundwater quality and high potential health risks in the Datong Basin, northern China: Research from published data. *Environ. Geochem. Health* **2021**, *43*, 791–812. [CrossRef] [PubMed]

63. Bhattacharya, P.; Jacks, G.; Jana, J.; Sracek, A.; Gustafsson, J.; Chatterjee, D. Geochemistry of the Holocene alluvial sediments of Bengal Delta Plain from West Bengal, India: Implications on arsenic contamination in groundwater. *Groundw. Arsen. Contam. Bengal Delta Plain Bangladesh* **2001**, *3084*, 21–40.

64. Reza, A.S.; Jean, J.-S.; Lee, M.-K.; Yang, H.-J.; Liu, C.-C. Arsenic enrichment and mobilization in the Holocene alluvial aquifers of the Chapai-Nawabganj district, Bangladesh: A geochemical and statistical study. *Appl. Geochem.* **2010**, *25*, 1280–1289. [CrossRef]

65. Lee, M.K.; Griffin, J.; Saunders, J.; Wang, Y.; Jean, J.S. Reactive transport of trace elements and isotopes in the Eutaw coastal plain aquifer, Alabama. *J. Geophys. Res. Biogeosci.* **2007**, *112*. [CrossRef]

66. Bhattacharya, P.; Chatterjee, D.; Jacks, G. Occurrence of arsenic-contaminatedGroundwater in alluvial aquifers from Delta plains, eastern India: Options for safe drinking water supply. *Int. J. Water Resour. Dev.* **1997**, *13*, 79–92. [CrossRef]

67. Kumar, M.; Ramanathan, A.; Mukherjee, A.; Verma, S.; Rahman, M.M.; Naidu, R. Hydrogeo-morphological influences for arsenic release and fate in the central Gangetic Basin, India. *Environ. Technol. Innov.* **2018**, *12*, 243–260. [CrossRef]

68. Piper, A.M. A graphic procedure in the geochemical interpretation of water-analyses. *Eos Trans. Am. Geophys. Union* **1944**, *25*, 914–928. [CrossRef]

69. Kumar, P.S. Interpretation of groundwater chemistry using piper and Chadha's diagrams: A comparative study from Perambalur Taluk. *Elixir Geosci.* **2013**, *54*, 12208–12211.

70. Saha, S.; Reza, A.S.; Roy, M.K. Hydrochemical evaluation of groundwater quality of the Tista floodplain, Rangpur, Bangladesh. *Appl. Water Sci.* **2019**, *9*, 198. [CrossRef]

71. Nag, S. Quality of groundwater in parts of ARSA block, Purulia District, West Bengal. *Bhu-Jal* **2009**, *4*, 58–64.

72. Sajil Kumar, P.; James, E. Identification of hydrogeochemical processes in the Coimbatore district, Tamil Nadu, India. *Hydrol. Sci. J.* **2016**, *61*, 719–731. [CrossRef]

73. Gibbs, R.J. Mechanisms controlling world water chemistry. *Science* **1970**, *170*, 1088–1090. [CrossRef]

74. Mattos, J.B.; Cruz, M.J.M.; De Paula, F.C.F.; Sales, E.F. Spatio-seasonal changes in the hydrogeochemistry of groundwaters in a highland tropical zone. *J. S. Am. Earth Sci.* **2018**, *88*, 275–286. [CrossRef]

75. Zhang, X.; Zhao, R.; Wu, X.; Mu, W. Hydrogeochemistry, identification of hydrogeochemical evolution mechanisms, and assessment of groundwater quality in the southwestern Ordos Basin, China. *Environ. Sci. Pollut. Res.* **2021**, *29*, 901–921. [CrossRef] [PubMed]

76. Khattak, S.A.; Rashid, A.; Tariq, M.; Ali, L.; Gao, X.; Ayub, M.; Javed, A. Potential risk and source distribution of groundwater contamination by mercury in district Swabi, Pakistan: Application of multivariate study. *Environ. Dev. Sustain.* **2021**, *23*, 2279–2297. [CrossRef]

77. Li, X.; Wu, H.; Qian, H.; Gao, Y. Groundwater chemistry regulated by hydrochemical processes and geological structures: A case study in Tongchuan, China. *Water* **2018**, *10*, 338. [CrossRef]

78. Das, N.; Patel, A.K.; Deka, G.; Das, A.; Sarma, K.P.; Kumar, M. Geochemical controls and future perspective of arsenic mobilization for sustainable groundwater management: A study from Northeast India. *Groundw. Sustain. Dev.* **2015**, *1*, 92–104. [CrossRef]

79. Noor, S.; Rashid, A.; Javed, A.; Khattak, J.A.; Farooqi, A. Hydrogeological properties, sources provenance, and health risk exposure of fluoride in the groundwater of Batkhela, Pakistan. *Environ. Technol. Innov.* **2022**, *25*, 102239.

80. Kumar, M.; Kumari, K.; Singh, U.K.; Ramanathan, A. Hydrogeochemical processes in the groundwater environment of Muktsar, Punjab: Conventional graphical and multivariate statistical approach. *Environ. Geol.* **2009**, *57*, 873–884. [CrossRef]

81. Datta, P.; Bhattacharya, S.; Tyagi, S. 18O studies on recharge of phreatic aquifers and groundwater flow-paths of mixing in the Delhi area. *J. Hydrol.* **1996**, *176*, 25–36. [CrossRef]

82. Rashid, A.; Khattak, S.A.; Ali, L.; Zaib, M.; Jehan, S.; Ayub, M.; Ullah, S. Geochemical profile and source identification of surface and groundwater pollution of District Chitral, Northern Pakistan. *Microchem. J.* **2019**, *145*, 1058–1065. [CrossRef]

83. Chotpantarat, S.; Amasvata, C. Influences of pH on transport of arsenate (As5+) through different reactive media using column experiments and transport modeling. *Sci. Rep.* **2020**, *10*, 1–13. [CrossRef] [PubMed]

84. Li, P.; Qian, H.; Wu, J.; Zhang, Y.; Zhang, H. Major ion chemistry of shallow groundwater in the Dongsheng Coalfield, Ordos Basin, China. *Mine Water Environ.* **2013**, *32*, 195–206. [CrossRef]

85. Rashid, A.; Guan, D.-X.; Farooqi, A.; Khan, S.; Zahir, S.; Jehan, S.; Khattak, S.A.; Khan, M.S.; Khan, R. Fluoride prevalence in groundwater around a fluorite mining area in the flood plain of the River Swat, Pakistan. *Sci. Total Environ.* **2018**, *635*, 203–215. [CrossRef]

86. Rashid, A.; Khan, S.; Ayub, M.; Sardar, T.; Jehan, S.; Zahir, S.; Khan, M.S.; Muhammad, J.; Khan, R.; Ali, A. Mapping human health risk from exposure to potential toxic metal contamination in groundwater of Lower Dir, Pakistan: Application of multivariate and geographical information system. *Chemosphere* **2019**, *225*, 785–795. [CrossRef]

87. Zhang, Y.; He, Z.; Tian, H.; Huang, X.; Zhang, Z.; Liu, Y.; Xiao, Y.; Li, R. Hydrochemistry appraisal, quality assessment and health risk evaluation of shallow groundwater in the Mianyang area of Sichuan Basin, southwestern China. *Environ. Earth Sci.* **2021**, *80*, 1–16. [CrossRef]

88. Rashid, A.; Farooqi, A.; Gao, X.; Zahir, S.; Noor, S.; Khattak, J.A. Geochemical modeling, source apportionment, health risk exposure and control of higher fluoride in groundwater of sub-district Dargai, Pakistan. *Chemosphere* **2020**, *243*, 125409. [CrossRef]

89. Liu, G.; Ma, F.; Liu, G.; Guo, J.; Duan, X.; Gu, H. Quantification of water sources in a coastal gold mine through an end-member mixing analysis combining multivariate statistical methods. *Water* **2020**, *12*, 580. [CrossRef]

90. Bhatti, Z.I.; Ishtiaq, M.; Khan, S.A.; Nawab, J.; Ghani, J.; Ullah, Z.; Khan, S.; Baig, S.A.; Muhammad, I.; Din, Z.U. Contamination level, source identification and health risk assessment of potentially toxic elements in drinking water sources of mining and non-mining areas of Khyber Pakhtunkhwa, Pakistan. *J. Water Health* **2022**, *20*, 1343–1363. [CrossRef]

91.   Agoubi, B.; Kharroubi, A.; Abida, H. Geochemical assessment of environmental impact on groundwater quality in coastal arid area, south eastern Tunisia. *J. Env. Sci. Eng. Technol.* **2014**, *2*, 35–46. [CrossRef]

92.   Kumar, A.; Singh, C.K. Characterization of hydrogeochemical processes and fluoride enrichment in groundwater of south-western Punjab. *Water Qual. Expo. Health* **2015**, *7*, 373–387. [CrossRef]

93.   Heydarirad, L.; Mosaferi, M.; Pourakbar, M.; Esmailzadeh, N.; Maleki, S. Groundwater salinity and quality assessment using multivariate statistical and hydrogeochemical analysis along the Urmia Lake coastal in Azarshahr plain, North West of Iran. *Environ. Earth Sci.* **2019**, *78*, 1–16. [CrossRef]

94.   Abu-Alnaeem, M.F.; Yusoff, I.; Ng, T.F.; Alias, Y.; Raksmey, M. Assessment of groundwater salinity and quality in Gaza coastal aquifer, Gaza Strip, Palestine: An integrated statistical, geostatistical and hydrogeochemical approaches study. *Sci. Total. Environ.* **2018**, *615*, 972–989. [CrossRef] [PubMed]

95.   EPA, Risk Based Screening Table. Composite Table: Summary Tab 0615, 2015. Available online: http://www2.epa.gov/risk/riskbasedscreeningtablegeneric%0Atables (accessed on 18 October 2022).

96.   Ram, A.; Tiwari, S.; Pandey, H.; Chaurasia, A.K.; Singh, S.; Singh, Y. Groundwater quality assessment using water quality index (WQI) under GIS framework. *Appl. Water Sci.* **2021**, *11*, 1–20. [CrossRef]